

**REGIONAL, SINGLE POINT,
AND GLOBAL BLOW-UP FOR THE FOURTH-ORDER
POROUS MEDIUM TYPE EQUATION WITH SOURCE**

V.A. GALAKTIONOV

ABSTRACT. Blow-up behaviour for the fourth-order quasilinear porous medium equation with source,

$$(0.1) \quad u_t = -(|u|^n u)_{xxxx} + |u|^{p-1} u \quad \text{in } \mathbb{R} \times \mathbb{R}_+, \quad n > 0, \quad p > 1,$$

is studied. Countable and finite families of similarity blow-up patterns of the form

$$u_S(x, t) = (T - t)^{-\frac{1}{p-1}} f(y), \quad \text{where } y = x/(T - t)^\beta, \quad \beta = \frac{p-(n+1)}{4(p-1)},$$

which blow-up as $t \rightarrow T^- < \infty$, are described. These solutions explain key features of regional (for $p = n + 1$), single point ($p > n + 1$), and global ($p \in (1, n + 1)$) blow-up. The concepts and various variational, bifurcation, and numerical approaches for revealing the structure and multiplicities of such blow-up patterns are presented.

1. INTRODUCTION: BLOW-UP REACTION-DIFFUSION MODELS

1.1. On classic second-order blow-up models and higher-order diffusion. Blow-up phenomena as intermediate asymptotics and approximations of highly nonstationary processes are common and well known in various areas of mechanics and physics. The origin of intensive systematic studies of such nonlinear effects was gas dynamics (since the end of the 1930s and 1940s) supported later in the 1960s by plasma physics (wave collapse) and nonlinear optics (self-focusing phenomena). Nevertheless, it was *reaction-diffusion theory* that exerted the strongest influence on mathematical blow-up research since the 1970s. It is not an exaggeration to say that reaction-diffusion theory proposed basic and nowadays canonical models, which eventually led to qualitative and rigorous description of principles of formation of blow-up and other singularities in nonlinear PDEs.

Finite-time blow-up singularities lie in the heart of several principal problems of PDE theory concerning existence, uniqueness, optimal regularity, and free-boundary propagation. The role of blow-up analysis in nonlinear PDE theory will increase when more complicated classes of higher-order degenerate parabolic, hyperbolic, nonlinear dispersion, and other equations of interest are involved in the framework of massive mathematical research and application. For such general classes of equations with typically non-potential,

Date: October 30, 2018.

1991 Mathematics Subject Classification. 35K55, 35K65.

Key words and phrases. Higher-order quasilinear parabolic equation, finite propagation, blow-up, similarity solutions, variational operators, branching.

Submitted to: JPDE, September, 2008.

non-divergent, and non-monotone operators (see classic monographs by Berger [2] and Krasnosel'skii–Zabreiko [31] for fundamentals of nonlinear operator theory), applications of many known classic techniques associated with some remarkable and famous specific PDEs become non-aplicable, so that a principally new methodology and even philosophy of nonlinear PDEs via blow-up analysis should play a part.

REACTION-DIFFUSION MODELS WITH BLOW-UP. The second-order quasilinear reaction-diffusion equations from combustion theory are widely used in the mathematical literature and many applications. This class of parabolic PDEs of principal interest in the twentieth century includes classic models beginning with the *Frank-Kamenetskii equation* with exponential nonlinearity (*solid fuel model*, 1938 [47]),

$$(1.1) \quad \begin{aligned} u_t &= \Delta u + e^u, \\ u_t &= \Delta u + u^p, \\ u_t &= \Delta(u^{n+1}) + u^p, \\ u_t &= \nabla \cdot (|\nabla u|^n \nabla u) + u^p, \end{aligned}$$

etc., where $n > 0$ and $p > 1$ are fixed exponents, and similar equations with more general nonlinearities. Due to the superlinear behaviour of the source terms e^u or u^p as $u \rightarrow +\infty$, these PDEs are known to create finite-time blow-up in the sense that a bounded solution ceases to exist and

$$(1.2) \quad \sup_{x \in \mathbb{R}} u(x, t) \rightarrow +\infty \quad \text{as} \quad t \rightarrow T^- < \infty.$$

If blow-up happens, the first key question is the behaviour of solutions as $t \rightarrow T^-$ that reflects both mathematical and physical-mechanical essence of these phenomena. Such singular limits create a class of one of the most difficult asymptotic problems in nonlinear PDE theory. The internal structure of these blow-up singularities can be rather complicated even for simplest combustion models in (1.1). It is worth mentioning that a full classification of the blow-up patterns is still not available for the last two *quasilinear* equations in this list.

In combustion modelling, the blow-up phenomena (1.2) are treated as *adiabatic explosions* (first results were due to Todes, 1933, in an ODE model), as an extremal type of instabilities in such nonlinear systems. The research in the area of blow-up combustion processes had been essentially intensified since the 1970s, when blow-up ideas first time penetrated key principles of the Laser Fusion (E. Teller's famous Report of 1972 on possibility of blow-up shockless compression of a D-T drop); see surveys in [26, p. 401] and [24, § 1.2]. There exists a huge amount of mathematical papers devoted to various aspects of blow-up and other singularity behaviour in parabolic equations and systems. We refer to monographs [1, 19, 27, 35, 40, 41], where detailed structures of blow-up are mainly studied and described for second-order reaction-diffusion PDEs. In [34], a systematic nonlinear capacity approach is developed to prove finite-time blow-up for wide classes of nonlinear evolution PDEs and systems of various orders and types. In [25, Ch. 3–5], blow-up structures for higher-order parabolic, hyperbolic, and nonlinear dispersion equations are treated by means of exact solutions on invariant subspaces for nonlinear operators.

First study and classification of finite families of single point blow-up patterns ($p > n + 1$) for the second-order counterpart

$$(1.3) \quad u_t = (u^{n+1})_{xx} + u^p \quad (u \geq 0)$$

have been known since 1970s. Basic new ideas of blow-up and heat localization for (1.3) were developed by Kurdyumov and his Russian School of blow-up regimes. See key references, main results, and history in [41, Ch. 4].

HIGHER-ORDER DIFFUSION AND STRUCTURE OF BLOW-UP. Much less is known still on formation of blow-up singularities in parabolic PDEs with higher-order diffusion that is also of essential demand in modern application. Even simplest PDEs such as the *extended Frank-Kamenetskii equation* in one dimension,

$$(1.4) \quad u_t = -u_{xxxx} + e^u \quad (\text{or} \quad u_t = u_{xxxxxx} + e^u),$$

and their counterparts with power source

$$(1.5) \quad u_t = -u_{xxxx} + |u|^{p-1}u \quad (\text{or} \quad u_t = u_{xxxxxx} + |u|^{p-1}u),$$

reveal several principally new asymptotic blow-up phenomena demanding novel mathematical approaches; see details in [9, 18]. Similar difficulties occur for the model equation from the *Semenov-Rayleigh-Benard problem* with the leading operator of the form

$$(1.6) \quad u_t = -u_{xxxx} + \beta[(u_x)^3]_x + e^u \quad (\beta \geq 0);$$

see [28]. The mathematical difficulties in understanding the ODE and PDE patterns increase dramatically with the order of differential diffusion operators in the equations. Interesting *regional blow-up* (see a definitions below) and oscillatory properties [10] are exhibited by a semilinear diffusion equation with “almost linear” logarithmic source term

$$(1.7) \quad u_t = -u_{xxxx} + u \ln^4 |u|.$$

There are just a few examples of higher-order parabolic reaction-diffusion PDEs with reasonably well-understood (but still not fully proved!) blow-up singularities. On the other hand, as we have mentioned, the techniques for proving global nonexistence of solutions are already available and cover a variety of nonlinear evolution equations of arbitrary orders; see [34]. Note that all the above models (1.4)–(1.7) are semilinear and do not admit blow-up patterns with finite propagation (i.e., with finite interfaces) and hence with *free boundaries* that are of special interest in PDE and ODE theory.

1.2. Fourth-order PME-type equation with source: on the model, techniques, and main results. In the present paper, we propose and study self-similar blow-up for the following *fourth-order porous medium equation with source* (PME–4 with source) :

$$(1.8) \quad \boxed{u_t = \mathbf{A}(u) \equiv -(|u|^n u)_{xxxx} + |u|^{p-1}u \quad \text{in } \mathbb{R} \times \mathbb{R}_+,}$$

where $n > 0$ and $p > 1$. For $n = 0$, this gives the semilinear equation (1.5) describing single point blow-up for all $p > 1$, [9]. For $n > 0$, blow-up phenomena and the corresponding mathematics for (1.8) are unknown and clearly become more involved.

We consider for (1.8) the Cauchy problem with bounded compactly supported data

$$(1.9) \quad u(x, 0) = u_0(x) \quad \text{in } \mathbb{R}.$$

Unlike the well-known from the 1980s *thin film equations* (TFEs) (see (1.15) below), the PDE (1.8) contains a fully divergent, monotone, and potential, differential operator. Moreover, (1.8) is a gradient system and admits strong estimates via multiplication by $(|u|^n u)_t$ in L^2 . The PME operator is potential in the metric of H^{-2} and is also monotone, so local existence of a unique continuous solution follows from classic theory of monotone operators; see [33, Ch. 2]. Finite propagation in the PDE (1.8) is proved by energy estimates via Saint–Venant’s principle; see various techniques in [3] and more recent results in [42] and also a survey in [24] for further references.

Global nonexistence results for PDEs like (1.8) are known from the beginning of the 1980s; see [17]. Concerning more recent results, let us mention that any solution of the Cauchy problem for

$$u_t = -\Delta^2(|u|^n u) + |u|^p \quad \text{in } \mathbb{R}^N \times \mathbb{R}_+, \quad u(x, 0) = u_0(x) \quad \text{in } \mathbb{R}^N$$

(recall the difference in the source term $|u|^p$ of the equation, which is associated with the nonlinear capacity method) blows up in the *subcritical Fujita range*

$$n + 1 < p \leq p_0 = n + 1 + \frac{4}{N}, \quad \text{provided that } \int u_0 > 0$$

(the first condition $n + 1 < p$ is also purely technical); see [12] for a brief simple exposition of the method and [34] for a systematic treatment.

It turns out that studying and proper understanding of higher-order models such as (1.8) demand completely different and more difficult mathematics, and, often, the known mathematical methods of classic nonlinear operator theory are not sufficient to answer some even basic and principal questions arisen. In other cases, tremendous efforts are necessary to justify their applicability for the nonlinear higher-order non-potential and non-variational operators involved. As happened before for the classic combustion model (1.3), complicated blow-up singularities for (1.8) hopefully are helping to initiate new mathematical directions that will take a long time to be proper developed. Several open problems appear that are stated throughout the text. Some of them are extremely difficult so the author just states and discusses these without specific mathematical efforts to solve.

LOCAL PROBLEM: OSCILLATORY SIGN-CHANGING BEHAVIOUR AT FINITE INTERFACES.

It is curious that though the principal fact on the oscillatory behaviour of solutions close to interfaces of the pure *fourth-order PME* (PME–4)

$$(1.10) \quad u_t = -(|u|^n u)_{xxxx} \quad (n > 0)$$

was rigorously established (together with existence and uniqueness of the Zel’dovich–Kompaneetz–Barenblatt source-type solutions) by Bernis [4] (1988) and in Bernis–McLeod [6] (1991), a detailed generic structure of such oscillations for (1.10) was not still fully addressed in mathematical literature. This was one of the principle open problem of local theory of higher-order PMEs. Therefore, we begin our analysis with this local oscillatory phenomenon that is also key for some similarity blow-up profiles:

(0) oscillatory behaviour of solutions near interfaces (Section 3).

GLOBAL BLOW-UP PROBLEMS: PATTERNS OF S-, LS-, AND HS-REGIMES. Concerning further evolution properties of (1.8), one of the main mathematical problems and difficulties is associated with the description and classification of blow-up patterns occurring in finite time. We reveal three classes of similarity blow-up for (1.8) in the ranges:

(i) $p = n + 1$, *regional blow-up* or *S-regime of blow-up* in Kurdyumov’s terminology [41, Ch. 4] (Section 5): this means that the solutions blows up as $t \rightarrow T^-$ in a bounded *localization domain*;

(ii) $p > n + 1$, *single point blow-up* or *LS-regime* (Section 6): the *final-time profile* $|u(x, t)| \rightarrow \infty$ as $t \rightarrow T^-$ at a single point and is uniformly bounded away from it; and

(iii) $p \in (1, n + 1)$, *global blow-up* or *HS-regime* (Section 7): $|u(x, t)| \rightarrow \infty$ as $t \rightarrow T^-$ uniformly on any compact subset in x .

In all the three cases, we detect the first p_0 -branch of F_0 -similarity profiles, which are expected to be *evolutionary (structurally) stable*, i.e., describe generic formation of blow-up singularities for the PDE (1.8). We present no proof (it is assumed to be very difficult) and no numerical evidence (a PDE modelling is then necessary that is out of our goals and reach here), and rely on our previous experience.

For $p \in (1, n + 1]$, the similarity patterns are shown to be *compactly supported* and oscillatory near interfaces, while for $p > n + 1$ they are not. It is also crucial that, in the case of regional blow-up for $p = n + 1$, the problem for similarity profiles becomes *variational*. Therefore, in Section 5, we detect countable families of various compactly supported similarity solutions by Lusternik–Schnirel’man category theory [31, § 57] and spherical fibering approach [38, 39]. Our rather natural and practical approach is *to use variational families of similarity profiles for $p = n + 1$ as the origin of p -branches for $p \neq n + 1$ appeared at the branching point $p = n + 1$* . In other words, the continuation in the parameter p makes it possible to observe and classify several blow-up patterns and p -branches in the non-variational cases $p > n + 1$ and $p < n + 1$. In Sections 6 and 7, we present typical p -bifurcation (branching) diagrams. For the higher-order ODEs appeared, several results are essentially based on refined numerical experiments (by using standard codes supplied **MatLab**), which often become the only tool to check global extensibility properties of various branches of similarity profiles. We do not think that, in a certain generality, all of these conclusions can be justified completely rigorously.

It is worth mentioning another fruitful approach to use the analogy with the linear bi-harmonic equation

$$(1.11) \quad u_t = -u_{xxxx} + u \quad \text{in} \quad \mathbb{R} \times \mathbb{R}_+,$$

which is obtained from (1.8) by both limits $n \rightarrow 0$ and $p \rightarrow 1$. A countable set of exponential patterns for (1.11) will be described on the basis of spectral theory developed in Section 2.

1.3. On other PDEs with striking similarities of the blow-up results. The present research and main approaches are better understood in conjunction with the results in

[21], where another canonical fourth-order models of the p -Laplacian operator with source,

$$(1.12) \quad u_t = -(|u_{xx}|^n u_{xx})_{xx} + |u|^{p-1}u, \quad n > 0, \quad p > 1,$$

is studied. It turns out amazingly that several general conclusions on blow-up behaviour for (1.8) and (1.12) coincide, but the necessary mathematics is completely different in many key places (e.g., the local oscillatory behaviour and the L–S variational approach), since the diffusion operators works in distinct functional spaces, H^{-1} and L^2 respectively. However, even existing similarities for these two nonlinear PDEs are not that easy to detect, since the mathematics involved essentially differs and the common roots of analogous results are rather obscure still. We will refer and use some common results in [21] when necessary and appropriate. The main principles of classification of blow-up similarity patterns and branches are claimed to remain the same for higher-order PDEs of similar type, e.g., for the *sixth-order PME-type equation with source* (PME–6 with source)

$$(1.13) \quad u_t = (|u|^n u)_{xxxxx} + |u|^{p-1}u.$$

Moreover, further developing this paradoxical phenomenon of analogy, the author claims that a number of local and similarities and geometrically equivalent set of nonlinear eigenfunctions are available for nonlinear degenerate PDEs such as (these awkward and artificial examples are chosen for the sake of the argument; note that these are not that far from real applications currently needed)

$$(1.14) \quad u_{ttt} = (|u|^{n-1}u)_{xxxxxxx} + |u|^{p-1}u \quad \text{or} \quad u_{tttt} = (|u_{xxxx}|^n u_{xxxx})_{xxxx} - (|u|^{p-1}u)_{xx}.$$

These PDEs are even hardly classified being a mixture of parabolic (mainly this), as well as having some features of wave, and nonlinear dispersion types. Such equations can be shown to exhibit blow-up patterns with oscillatory finite interfaces, where the mathematics and patterns formation/classification remain similar but of course more involved.

1.4. On other higher-order PDEs with blow-up or extinction and finite interfaces. For convenience of the Reader and for completeness of our short survey on blow-up in nonlinear higher-order parabolic PDEs, the *interface* and *blow-up phenomena* are natural and most well-known for the degenerate unstable *thin film equations* (TFEs)

$$(1.15) \quad u_t = -(|u|^n u_{xx})_x - (|u|^{p-1}u)_{xx} \quad \text{with } n > 0, \quad p > 1.$$

Equations of this form admit non-negative solutions constructed by special sufficiently “singular” parabolic approximations of nonlinear coefficients that often lead to free-boundary problems. This direction was initiated by the pioneering paper [5] and was continued by many researchers; we refer to [32, 46] and the references therein. Blow-up similarity solutions of the fourth-order TFE (1.15) have been also well studied and understood; see [7, 8, 15, 43, 46], where further references on the mathematical properties of the models can be found. Oscillatory solutions and countable sets of blow-up patterns for this TFE were described in [15].

Interface and *extinction* behaviour occur for other reaction-absorption PDEs such as

$$(1.16) \quad u_t = -u_{xxxx} - |u|^{p-1}u$$

in the *singular* parameter range $p \in (-\frac{1}{3}, 1)$, where the absorption term $|u|^{p-1}u$ is not Lipschitz continuous at $u = 0$. This creates interesting evolution extinction phenomena and various sets of similarity patterns; see [20] and references therein.

2. FUNDAMENTAL SOLUTION AND SPECTRAL PROPERTIES FOR $n = 0$

These questions have been discussed in [21, § 3.3], so we briefly report on those auxiliary properties. Consider the linear *bi-harmonic equation* corresponding to $n = 0$,

$$(2.1) \quad u_t = -u_{xxxx} \quad \text{in } \mathbb{R} \times \mathbb{R}_+.$$

Its *fundamental solution* has the form

$$(2.2) \quad b(x, t) = t^{-\frac{1}{4}}F(y), \quad y = x/t^{\frac{1}{4}}, \quad \text{where}$$

$$(2.3) \quad \mathbf{B}F \equiv -F^{(4)} + \frac{1}{4}yF' + \frac{1}{4}F = 0 \quad \text{in } \mathbb{R}, \quad \text{with } \int F = 1.$$

The rescaled kernel $F = F(|y|)$ is radial, has exponential decay, oscillates as $|y| \rightarrow \infty$, and [14, p. 46]

$$(2.4) \quad |F(y)| \leq De^{-d|y|^{4/3}} \quad \text{in } \mathbb{R},$$

for some positive constant D and $d = 3 \cdot 2^{-11/3}$. The necessary spectral properties of the linear operator \mathbf{B} and the corresponding adjoint operator \mathbf{B}^* can be found in [13] for similar more general $2m$ th-order operators (see also [15, § 4]). In particular, \mathbf{B} is naturally defined in a weighted space $L^2_\rho(\mathbb{R})$, with $\rho(y) = e^{a|y|^{4/3}}$, where $a \in (0, 2d)$ is a constant, and has the discrete (point) spectrum

$$(2.5) \quad \sigma(\mathbf{B}) = \left\{ \lambda_l = -\frac{l}{4}, \quad l = 0, 1, 2, \dots \right\}.$$

The corresponding eigenfunctions are given by differentiating the kernel,

$$(2.6) \quad \psi_l(y) = \frac{(-1)^l}{\sqrt{l!}} F^{(l)}(y), \quad l = 0, 1, 2, \dots$$

The adjoint operator

$$(2.7) \quad \mathbf{B}^* = -D_y^4 - \frac{1}{4}yD_y$$

has the same spectrum (2.5) and eigenfunctions being generalized Hermite polynomials

$$(2.8) \quad \psi_l^*(y) = \frac{1}{\sqrt{l!}} \sum_{j=0}^{\lfloor -\lambda_l \rfloor} \frac{1}{j!} D_y^{4j} y^l, \quad l = 0, 1, 2, \dots,$$

which form a complete and closed set in $L^2_{\rho^*}(\mathbb{R})$, where $\rho^*(y) = \frac{1}{\rho(y)}$. The bi-orthonormality of eigenfunction sets holds:

$$(2.9) \quad \langle \psi_l, \psi_k^* \rangle = \delta_{lk},$$

where $\langle \cdot, \cdot \rangle$ denotes the standard (dual) scalar product in $L^2(\mathbb{R})$.

3. LOCAL ASYMPTOTIC PROPERTIES OF SOLUTIONS NEAR INTERFACES

We study the oscillatory behaviour of solutions of (1.8) close to interfaces.

3.1. Local properties of travelling waves (TWs). As customary, we use TWs solutions,

$$(3.1) \quad u(x, t) = f(y), \quad y = x - \lambda t,$$

to describe propagation properties for (1.8). Then $f(y)$ solves

$$(3.2) \quad -\lambda f' = -(|f|^n f)^{(4)} + |f|^{p-1} f.$$

By a local analysis near the interface, at which $f = 0$ (and, as we will see, also $f' = f'' = f''' = 0$ for all $n > 0$), it is not difficult to see that the higher-order term $|f|^{p-1} f$ on the right-hand side is negligible. Therefore, near moving interfaces, we consider the simpler equation

$$(3.3) \quad (|f|^n f)''' = -f \quad \text{for } y > 0, \quad f(0) = 0,$$

which is obtained on integration once. Here we set $\lambda = -1$ by scaling for propagating waves. It is convenient to use the natural change

$$(3.4) \quad F = |f|^n f \quad \Longrightarrow \quad F''' = -|F|^{-\frac{n}{n+1}} F.$$

We describe oscillatory solutions of changing sign of (3.4), with zeros concentrating at the given interface point $y = 0^+$. *Q.v.* the pioneering papers by Bernis and McLeod [4, 6].

Actually, we are going to give a sharp description of the behaviour of the solutions close to interfaces. By the scaling invariance of (3.4), we look for solutions of the form

$$(3.5) \quad F(y) = y^\mu \varphi(s), \quad s = \ln y, \quad \text{where } \mu = \frac{3(n+1)}{n} > 3 \text{ for } n > 0,$$

where $\varphi(s)$ is the *oscillatory component*. Substituting (3.5) into (3.4) yields the ODE

$$(3.6) \quad P_3(\varphi) = -|\varphi|^{-\frac{n}{n+1}} \varphi.$$

Linear differential operators P_k are given by the recursion (see [25, p. 140])

$$\begin{aligned} P_{k+1}(\varphi) &= P'_k(\varphi) + (\mu - k)P_k(\varphi), \quad k \geq 0; \quad P_0(\varphi) = \varphi, \quad \text{so that} \\ P_1(\varphi) &= \varphi' + \mu\varphi, \quad P_2(\varphi) = \varphi'' + (2\mu - 1)\varphi' + \mu(\mu - 1)\varphi, \\ P_3(\varphi) &= \varphi''' + 3(\mu - 1)\varphi'' + (3\mu^2 - 6\mu + 2)\varphi' + \mu(\mu - 1)(\mu - 2)\varphi, \quad \text{etc.} \end{aligned}$$

In view of (3.5), we look for uniformly bounded global solutions $\varphi(s)$ that are defined for all $s \ll -1$, i.e., can be extended to the interface at $y = 0^+$. The best candidates for such global orbits of (3.6) are periodic solutions $\varphi_*(s)$ that are defined for all $s \in \mathbb{R}$. Indeed, they can describe suitable (and, possibly, generic) connections with the interface at $s = -\infty$. Existence of such a periodic solution $\varphi_*(s)$ of (3.6) can be achieved by shooting arguments; see details in [16, § 7], where further references concerning periodic orbits of higher-order ODEs are given. Uniqueness of φ_* remains an open mathematical problem, though was always confirmed numerically.

Figure 1 shows fast convergence to such a unique (numerically) stable periodic solution of (3.6) for various $n > 0$. These numerics are obtained by using the ODE solver `ode45` **MatLab** with enhanced tolerances and a regularization in the singular term up to 10^{-12} ; see (5.17) and more comments in Section 5, where more advanced numerical techniques

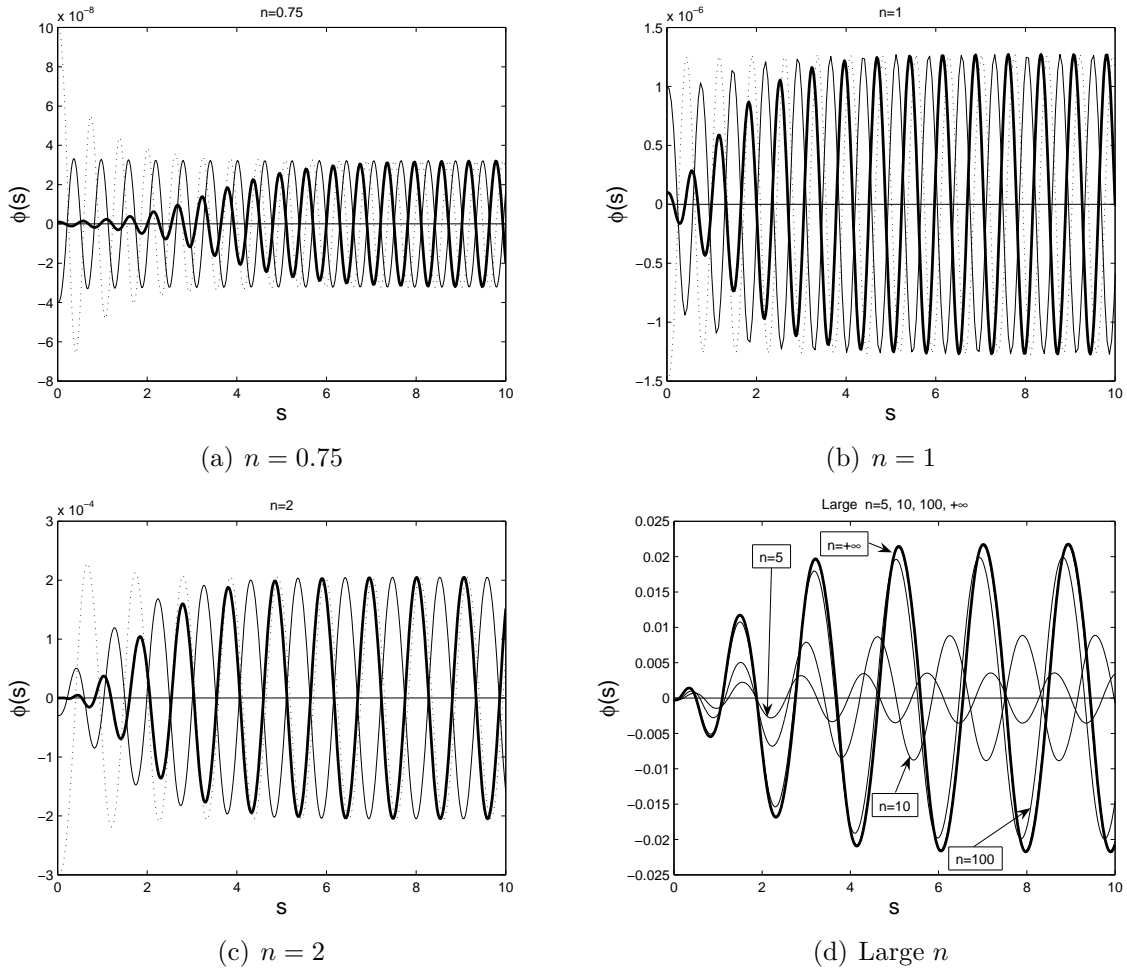


FIGURE 1. Convergence to a stable periodic orbit (3.4) for various $n > 0$.

for solving boundary-value problems are employed. Different curves therein correspond to different Cauchy data $\varphi(0)$, $\varphi'(0)$, $\varphi''(0)$ prescribed at $s = 0$. For n smaller than $\frac{3}{4}$, the oscillatory component gets extremely small, so an extra scaling is necessary, which is explained in [16, § 7.3]. A more accurate passage to the limit $n \rightarrow 0$ in (3.6) is done there in § 7.6 and in Appendix B. In (d), we also present the periodic solution for $n = +\infty$ where (3.6) takes a simpler form,

$$P_3(\varphi) = -\text{sign } \varphi.$$

Finally, given the periodic $\varphi_*(s)$ of (3.6), as a natural way to approach the interface point $y_0 = 0$ according to (3.5), we have that the ODE (3.3) and, asymptotically, (3.2), generate at the singularity set $\{f = 0\}$

(3.7) a 2D local asymptotic bundle with parameters y_0 and phase shift in $s \mapsto s + s_0$.

This two-dimensional bundle will be shown to be sufficient for matching with, typically, two boundary conditions that generate blow-up patterns.

3.2. Non-oscillatory case $\lambda > 0$: 1D bundle of non-oscillatory asymptotics. For $\lambda = +1$, we have the opposite sign in the ODE

$$(3.8) \quad P_3(\varphi) = |\varphi|^{-\frac{n}{n+1}}\varphi,$$

which admits two equilibria

$$(3.9) \quad \varphi_{\pm} = \pm[\mu(\mu-1)(\mu-2)]^{-\frac{n+1}{n}}.$$

Let us check the dimension of their stable manifolds as $s \rightarrow +\infty$ and, most importantly, $s \rightarrow -\infty$, which corresponds to approaching the interface. Note that, for (3.6) the trivial equilibrium $\varphi_0 = 0$ is evidently unstable in both directions with empty stable manifolds (in view of the non-Lipschitz nonlinearity at $\varphi = 0$ on the right-hand side).

Thus, by standard linearization, it follows that both are stable as $s \rightarrow +\infty$: setting $\varphi = \varphi_+ + Y$ yields the linear ODE

$$(3.10) \quad \mathbf{P}Y \equiv \left[P_3 - \frac{1}{n+1} \mu(\mu-1)(\mu-2)I \right] Y = 0.$$

The characteristic equation by plugging $Y = e^{\lambda s}$ into (3.10) takes the form

$$(3.11) \quad p(\lambda) \equiv \lambda^3 + 3(\mu-1)\lambda + (3\mu^2 - 6\mu + 2)\lambda + 3(\mu-1)(\mu-2) = 0, \quad \text{where}$$

$$p(0) = 3(\mu-1)(\mu-2) > 0, \quad p'(\lambda) = 0 \text{ at } \lambda_{\pm} = \frac{1}{3}[-3(\mu-1) \pm \sqrt{3}] < 0.$$

It follows that all characteristic values of \mathbf{P} satisfy

$$(3.12) \quad \text{Re } \lambda_k < 0, \quad k = 1, 2, 3.$$

Figure 2(a) also confirms that as $s \rightarrow +\infty$ the equilibria (3.9) are stable. In (b), which gives the enlarged image of the behaviour from (a) close to $\varphi = 0$, we observe a changing sign orbit, which is not a periodic one. Therefore, this cannot be extended as a bounded solution up to the interface at $s = -\infty$. There are many other similar ODEs, where such behaviour between two equilibria is periodic; cf. [25, p. 143].

In a whole, these results confirm that for $\lambda > 0$, the TWs *are not oscillatory at interfaces*, so that, formally, this *backward* propagation can be performed by positive solutions. On the other hand, (3.12) establishes that the stable manifold of equilibria φ_{\pm} as $s \rightarrow -\infty$ (i.e., towards the interface) is empty, so that unlike (3.7), for $\lambda = +1$,

$$(3.13) \quad \exists \text{ a 1D local asymptotic bundle with parameter } y_0.$$

One can see from (3.5) that these positive asymptotics are given by (for fixed $\lambda = +1$ which has been scaled out as a non-essential parameter)

$$(3.14) \quad f(y) = (y - y_0)^{\frac{3}{n}} [\mu(\mu-1)(\mu-2)]^{-\frac{1}{n}} (1 + o(1)) \quad \text{as } y \rightarrow y_0^+.$$

This 1D bundle is not enough for construction of typical global connections via two boundary conditions, so that the backward propagation is either not possible at all for almost all (a.a.) initial data in the Cauchy problem for (1.10), or it is not performed by TWs.

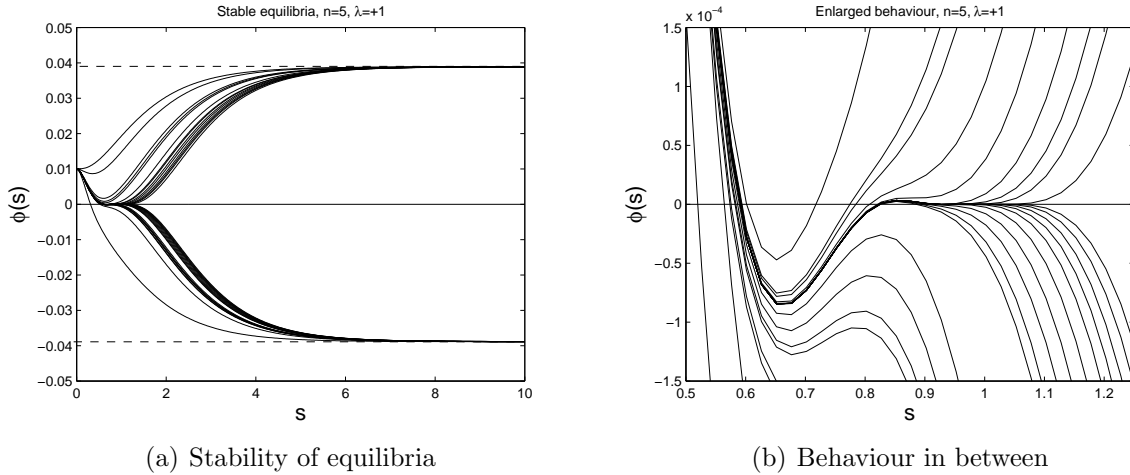


FIGURE 2. Non-oscillatory behaviour for the ODE (3.8) for $n = 5$; stability of equilibria (3.9) (a), and enlarged non-periodic behaviour in between, (b).

In other words, this shows that, for the PME-4 (1.10), the forward propagation of interfaces is common. Concerning the backward one, though existing for specific initial data, it is not plausible in general. Recall that for the standard PME

$$(3.15) \quad u_t = (|u|^n u)_{xx},$$

the backward propagation of non-negative solutions is completely prohibited by the Maximum Principle (by the straightforward comparison from below with slowly moving small TWs). For higher-order equations, these barrier techniques via comparison fail, but anyway, via the reduction of the bundle dimension in (3.13), we justify a similar phenomenon, which is now true not for *all*, but for *a.a.* initial data. It is worth mentioning that the PME (3.15) also admits oscillatory solutions near interfaces (see references and comments in [19, p. 30]). By Sturm's First Theorem on non-increase of the number of zeros, such behaviour is not generic for second-order parabolic PDEs in the sense that such solutions cannot appear from data with any finite number of sign changes.

4. BLOW-UP SIMILARITY SOLUTIONS: PROBLEM SETTING AND PRELIMINARIES

4.1. Posing the similarity problem. The parabolic PDE (1.8) admits the following similarity solutions with blow-up as $t \rightarrow T^-$:

$$(4.1) \quad u_S(x, t) = (T - t)^{-\frac{1}{p-1}} f(y), \quad y = x/(T - t)^\beta, \quad \text{with} \quad \beta = \frac{p-(n+1)}{4(p-1)}.$$

The rescaled profile $f(y)$ solves a quasilinear fourth-order ODE

$$(4.2) \quad \mathbf{A}(f) \equiv -(|f|^n f)^{(4)} - \beta y f' - \frac{1}{p-1} f + |f|^{p-1} f = 0 \quad \text{in} \quad \mathbb{R}.$$

Equation (4.2) has the constant equilibria

$$(4.3) \quad \pm f_*(p) = \pm(p-1)^{-\frac{1}{p-1}} \rightarrow \pm\infty \quad \text{as} \quad p \rightarrow 1^+.$$

For even solutions $f(y)$, symmetry conditions at the origin $y = 0$ are posed,

$$(4.4) \quad f'(0) = 0 \quad \text{and} \quad f'''(0) = 0 \quad (\text{if } f(0) \neq 0),$$

while for odd ones we impose the anti-symmetry ones

$$(4.5) \quad f(0) = 0 \quad \text{and} \quad f''(0) = 0.$$

A natural setting for the Cauchy problem assumes that, for $p \in (1, n + 1]$,

$$(4.6) \quad f(y) \text{ is sufficiently smooth and compactly supported.}$$

The actual regularity of $f(y)$ close to interfaces was determined in the previous section by the local asymptotic analysis. For $p > n + 1$, the solutions are not compactly supported.

The ODE (4.2) is a difficult fourth-order nonlinear equation, so that, in general, existence and multiplicity results for the above boundary-value problems reduce to complicated, at least, 2D shooting problems (recall (3.7) and two boundary conditions). This principally differs (4.2) from its second-order counterparts associated with the combustion model (1.3), where the most of the results admit either a clear phase-plane interpretation or reduce to 1D shooting in the presence of the Maximum Principle; see typical results and references in [41, Ch. 4]. Bearing in mind that, for the PME–6 with source (1.13), the parameter space of shooting will be 3D, we cannot rely on these geometric ideas, and have to use a principally different approach for reliable detecting multiple blow-up patterns. This will be variational approach to the case $p = n + 1$ plus p -branching approach for $p > n + 1$ and $p < n + 1$.

4.2. Blow-up self-similar profiles: preliminaries. We next study global compactly supported solutions of the ODE (4.2). For $p \leq n + 1$, the local interface analysis from Section 3 applies to (4.2). Indeed, close to the interface point $y = y_0 > 0$ of the similarity profile $f(y)$, the ODE (4.2) contains the same leading terms as in (3.3) and other linear two are negligible as $y \rightarrow y_0^-$.

It is key that, taking into account the local result (3.7) and bearing in mind the two boundary conditions in (4.4) or (4.5), we may expect that

$$(4.7) \quad \text{there exists not more than a countable set } \{f_k\} \text{ of solutions.}$$

This speculations assume a certain ‘‘analyticity’’ hypothesis concerning the dependence on parameters in the degenerate ODE (4.2), which is plausible but not easy to prove. Actually, this means that, relative to the parameter $p > 1$, we can expect at most a countable set of p -branches of solutions. To begin with, this is true for the linear case $n = 0$ and $p = 1$.

4.3. Countable set of similarity solutions for $n = 0$, $p = 1$, and homotopic connection. These questions are discussed in detail in [21, § 3.4], so we briefly comment that the linear PDE (1.11) has a *countable* set of patterns given by eigenfunctions (2.6):

$$(4.8) \quad u_l(x, t) = e^{-t} t^{-\frac{1+l}{4}} \psi_l\left(\frac{x}{t^{1/4}}\right), \quad l = 0, 1, 2, \dots$$

Our intention is to see how the blow-up similarity patterns (4.1) can be deformed as $n \rightarrow 0$ and $p \rightarrow 1$ to those in (4.8). Then (4.8) suggests that, for $n > 0$, there exists a countable

number of “branches” $\{f_i(y; n, p)\}$, which “bifurcate” from the point $\{n = 0, p = 1\}$. It is possible to observe the space-time structures in (4.8) in nonlinear blow-up analysis, where similar countable sets of patterns will be shown to exist; see [29]. We then say that the above two (linear for $n = 0, p = 1$ and nonlinear for $n > 0, p > 1$) asymptotic problems admit a continuous *homotopic* connection as $n \rightarrow 0, p \rightarrow 1$. See [21] for extra details.

5. REGIONAL BLOW-UP SIMILARITY PROFILES FOR $p = n + 1$

As in [21, § 4], the case $p = n + 1$ is simpler since $\beta = 0$, so (4.1) is a solution in separable variables

$$u(x, t) = (T - t)^{-\frac{1}{n}} f(x).$$

Then $f = f(y)$ (we continue to use y as the independent spatial variable for application to $p \neq n + 1$) solves an autonomous fourth-order ODE of the form

$$(5.1) \quad \mathbf{A}(f) \equiv -(|f|^n f)^{(4)} - \frac{1}{n} f + |f|^n f = 0 \quad \text{in } \mathbb{R}.$$

We again use the same change as in (3.4),

$$(5.2) \quad |f|^n f = n^{-\frac{n+1}{n}} F \quad \implies \quad F^{(4)} = F - |F|^{-\frac{n}{n+1}} F \quad \text{in } \mathbb{R}.$$

This equation is much simpler than that in [21], and was studied in [23]. We briefly present the main conclusions that will play an important role for the cases $p > n + 1$ and $p < n + 1$ later on.

5.1. Variational setting. The operators in (5.2) are potential, so the problem admits a variational setting, so the solutions can be obtained as critical points of a C^1 functional of the form

$$(5.3) \quad E(F) = -\frac{1}{2} \int (F'')^2 dy + \frac{1}{2} \int F^2 dy - \frac{1}{\nu} \int |F|^\nu dy, \quad \text{where } \nu = \frac{n+2}{n+1} \in (1, 2).$$

We are interested in critical points in $W_2^2(\mathbb{R}) \cap L^2(\mathbb{R}) \cap L^\nu(\mathbb{R})$. Especially, we are interested in localized compactly supported solutions, so we choose a sufficiently large interval $B_R = (-R, R)$ and consider the variational problem for (5.3) in $W_{2,0}^2(B_R)$, where we assume Dirichlet boundary conditions at the end points $\partial B_R = \{\pm R\}$. By Sobolev embedding theorem, $W_{2,0}^2(B_R) \subset L^2(B_R)$ and in $L^{p+1}(B_R)$ compactly for any $p \geq 1$. Continuity of any bounded solution $F(y)$ is guaranteed by Sobolev embedding $H^2(\mathbb{R}) \subset C(\mathbb{R})$. We also need the following:

Proposition 5.1. *Let F be a continuous weak solution of the equation (5.2) such that*

$$(5.4) \quad F(y) \rightarrow 0 \quad \text{as } y \rightarrow \infty.$$

Then F is compactly supported in \mathbb{R} .

Proof. Consider the corresponding parabolic equation with the same elliptic operator,

$$(5.5) \quad w_t = -w_{xxxx} + w - |w|^{p-1} w \quad \text{in } \mathbb{R}_+ \times \mathbb{R}, \quad \text{where } p = \frac{1}{n+1} \in (0, 1),$$

with initial data $F(y)$. Setting $w = e^t \hat{w}$ yields the equation

$$(5.6) \quad \hat{w}_t = -\hat{w}_{xxxx} - e^{-\frac{n}{n+1}t} |\hat{w}|^{p-1} \hat{w},$$

where the operator is monotone in $L^2(\mathbb{R})$. Therefore, the CP with initial data F has a unique weak solution, [33, Ch. 2]. Thus, (5.5) has the unique solution $w(y, t) \equiv F(y)$. In the presence of the singular absorption $-|u|^{p-1}u$, with $p < 1$, there occurs the phenomenon of *instantaneous compactification* or *shrinking of the support* of the solution for any data satisfying (5.4) (or even for more general data in L^p -spaces). Such phenomena for quasilinear absorption-diffusion equations for $p < 1$ have been known since the 1970s. By energy estimates, similar results were proved for a number of quasilinear higher-order parabolic equations with non-Lipschitz absorption terms, [3, 42]. By the instantaneous compactification, the multiplier $e^{-\frac{n}{n+1}t}$ in the absorption in (5.6) changes nothing. \square

Thus, to revealing compactly supported patterns $F(y)$, we have to pose the problem in bounded sufficiently large intervals.

5.2. L–S theory and direct application of fibering method. Unlike [21, § 4], this application is more standard. Namely, we apply classic Lusternik–Schnirel’man (L–S) theory of calculus of variations [31, § 57] in the form of the fibering method [38, 39]. Then the number of critical points of the functional (5.3) depends on the *category* (or Krasnosel’skii’s *genus* [31, § 57]) of the functional subset, on which fibering is taking place. The critical points of $E(F)$ are obtained by the *spherical fibering* in the form

$$(5.7) \quad F = r(v)v \quad (r \geq 0),$$

where $r(v)$ is a scalar functional, and v belongs to the subset

$$(5.8) \quad \mathcal{H}_0 = \{v \in W_{2,0}^2(B_R) : H_0(v) \equiv -\int (v'')^2 dy + \int v^2 dy = 1\}.$$

The new functional

$$(5.9) \quad H(r, v) = \frac{1}{2}r^2 - \frac{1}{\nu}r^\nu \int |v|^\nu dy$$

has the absolute minimum point, where

$$(5.10) \quad H'_r \equiv r - r^{\nu-1} \int |v|^\nu dy = 0 \implies r_0(v) = \left(\int |v|^\nu dy\right)^{\frac{1}{2-\nu}},$$

at which $H(r_0(v), v) = -\frac{2-\nu}{2\nu} r_0^2(v)$. Introducing

$$(5.11) \quad \tilde{H}(v) = \left[-\frac{2\nu}{2-\nu} H(r_0(v), v)\right]^{\frac{2-\nu}{2}} \equiv \int |v|^\nu dy,$$

yields an even, non-negative, convex, and uniformly differentiable functional, to which L–S theory applies, [31, § 57]; see also [11, p. 353]. Following [39], searching for critical points of \tilde{H} in \mathcal{H}_0 , one needs to estimate the category ρ of the set \mathcal{H}_0 . The details on this notation and basic results can be found in Berger [2, p. 378]. Notice that the Morse index q of the quadratic form Q in Theorem 6.7.9 therein is the dimension of the space where the corresponding form is negatively definite. This includes all the multiplicities of eigenfunctions involved in the corresponding subspace.

For application, it is convenient to recall that utilizing Berger’s version [2, p. 368] of this minimax analysis of L–S category theory [31, p. 387], the critical values $\{c_k\}$ and the corresponding critical points $\{v_k\}$ are given by

$$(5.12) \quad c_k = \inf_{\mathcal{F} \in \mathcal{M}_k} \sup_{v \in \mathcal{F}} \tilde{H}(v),$$

where $\mathcal{F} \subset \mathcal{H}_0$ are closed sets, and \mathcal{M}_k denotes the set of all subsets of the form $BS^{k-1} \subset \mathcal{H}_0$, where S^{k-1} is a suitable sufficiently smooth $(k-1)$ -dimensional manifold (say, sphere) in \mathcal{H}_0 and B is an odd continuous map. Then each member of \mathcal{M}_k is of genus at least k (available in \mathcal{H}_0). It is also important to remind that the definition of genus [31, p. 385] assumes that $\rho(\mathcal{F}) = 1$, if no *component* of $\mathcal{F} \cup \mathcal{F}^*$, where $\mathcal{F}^* = \{v : -v \in \mathcal{F}\}$, is the *reflection* of \mathcal{F} relative to 0, contains a pair of antipodal points v and $v^* = -v$. Furthermore, $\rho(\mathcal{F}) = n$ if each compact subset of \mathcal{F} can be covered by, minimum, n sets of genus one.

According to (5.12), $c_1 \leq c_2 \leq \dots \leq c_{l_0}$, where $l_0 = l_0(R)$ is the category of \mathcal{H}_0 (see an estimate below) satisfying

$$(5.13) \quad l_0(R) \rightarrow +\infty \quad \text{as} \quad R \rightarrow \infty.$$

Roughly speaking, since the dimension of the sets \mathcal{F} involved in the construction of \mathcal{M}_k increases with k , this guarantees that the critical points delivering critical values (5.12) are all different.

It follows from (5.8) that the category $l_0 = \rho(\mathcal{H}_0)$ of the set \mathcal{H}_0 is equal to the number (with multiplicities) of the eigenvalues $\lambda_k > -1$ of the linear bi-harmonic operator,

$$(5.14) \quad -w^{(4)} = \lambda_k \psi, \quad \psi \in W_{2,0}^2(B_R).$$

Since the dependence of the spectrum on R is, obviously,

$$(5.15) \quad \lambda_k(R) = R^{-4} \lambda_k(1), \quad k = 0, 1, 2, \dots,$$

the category $\rho(\mathcal{H}_0)$ can be arbitrarily large for $R \gg 1$, (5.13) holds, and we obtain:

Proposition 5.2. *The ODE problem (5.2) has at least a countable set of different solutions denoted by $\{F_l, l \geq 0\}$, each one obtained as a critical point of the functional (5.3) in $W_{2,0}^2(B_R)$ with sufficiently large $R > 0$.*

5.3. First basic pattern and local structure of zeros. We next present numerical results concerning existence and multiplicity of solutions for equation (5.2). In Figure 3, we show the first basic pattern for (5.2) called the $F_0(y)$ for various $n \in [0.1, 100]$. Note that (5.2) admits a natural passage to the limit $n \rightarrow +\infty$ that gives the ODE

$$(5.16) \quad F^{(4)} = F - \text{sign } F \equiv \begin{cases} F - 1 & \text{for } F \geq 0, \\ F + 1 & \text{for } F < 0. \end{cases}$$

A unique oscillatory solution of (5.16) can be treated by an algebraic approach; cf. [16, § 7.4]. The solutions for $n = 1000$ or $n = +\infty$ practically do not differ from the last profile for $n = 100$ in Figure 3.

These profiles are constructed by **MatLab** by using a natural regularization in the singular term in (5.2),

$$(5.17) \quad F^{(4)} = F - (\varepsilon^2 + F^2)^{-\frac{n}{2(n+1)}} F \quad \text{in } \mathbb{R}.$$

Here, the regularization parameter ε and both absolute and relative tolerances in the **bvp4c** solver have been enhanced and took the values

$$(5.18) \quad \varepsilon = 10^{-10} \quad \text{and} \quad \text{Tols} = 10^{-10}.$$

This allows us also to reveal the refined local structure of multiple zeros at the interfaces. Figure 4 for $n = 1$ shows how the zero structure repeats itself in a self-similar manner from one zero to another in the usual linear scale.

In Figure 5, we present the results for $n = 1$ that show the oscillatory structure in the log-scale such as (3.5) with $y \mapsto y_0 - y$ and

$$(5.19) \quad \mu = \frac{4(n+1)}{n} \Big|_{n=1} = 8 \quad \implies \quad \ln |F(y)| = 8 \ln(y_0 - y) + \ln |\varphi_*(\ln(y_0 - y))| + \dots$$

(see also (5.23) below). This figure shows an “ ε -dynamic” formation of at least six-seven nonlinear zeros, when we decrease $\varepsilon = \text{Tols}$ from 10^{-3} (just two first nonlinear zeros; the rest correspond to the linear ones in (5.20)) to 10^{-10} (6-7 zeros are nonlinear). Observe a “concave” shape of the graph for the last $\varepsilon = 10^{-10}$, which is consistent with the log-shape in (5.19) (we claim that even a trace of the multiplier 8 can be distinguished by 6 zeros).

Further decrease of ε and Tols leads to quick divergence of `bvp4c` solver, which has the limit minimal Tols 10^{-13} , which is not that helpful in comparison with 10^{-10} achieved in Figure 5. The right-hand interface is then estimated as (it is quite a challenge to detect numerically the free-boundary point more accurately)

$$y_0 \approx 12.$$

The “nonlinear area” ends at $y \sim 11$ (due to the requires accuracy and ε -regularization), and next we observe the “linearized area” where (5.17) implies an exponential behaviour for $y \gg 1$ governed by the linearized ODE

$$(5.20) \quad F^{(4)} = -\varepsilon^{-\frac{n}{n+1}} F + \dots \quad \implies \quad F(y) \sim e^{-c_1 \varepsilon^{-\frac{n}{4(n+1)}}} \cos(c_2 \varepsilon^{-\frac{n}{4(n+1)}} y + c_3),$$

where c_k are constants and $c_1 > 0$. From $y \sim 12.5$ ($F \sim 10^{-12}$), the numerics are not reliable at all.

5.4. The first basic pattern $F_0(y)$: on the behaviour as $n \rightarrow 0$. In order to understand the continuous connection with the linear PDE (1.11) and other homotopy results, one needs to pass to the limit $n \rightarrow 0^+$ in the ODE (5.2). Figure 6 shows the behaviour of the first basic profile $F_0(y)$ for small $n = 10^{-1}, 10^{-2}, \dots, 10^{-7}$ (a), while (b) explains the behaviour of the maximum value $F_0(0)$ and around.

It follows from equation (5.2) that, for $n \approx 0^+$, close to the origin and uniformly on bounded intervals in y , the smooth solution $F_0(y)$ approaches an even function satisfying the linear homogeneous equation

$$(5.21) \quad F^{(4)} = 0 \quad \implies \quad F_0(y) \approx C_0(n) - A_0(n)y^2,$$

so that $F_0(y)$ essentially depends on small n . Here both unknown coefficients $C_0(n) \rightarrow C_0(0)$ and $A_0(n) \rightarrow 0$ are slightly oscillatory as $n \rightarrow 0$ (in view of the non-monotone behaviour in (5.23) near the interface), with

$$(5.22) \quad C_0(0) \approx 1.435\dots$$

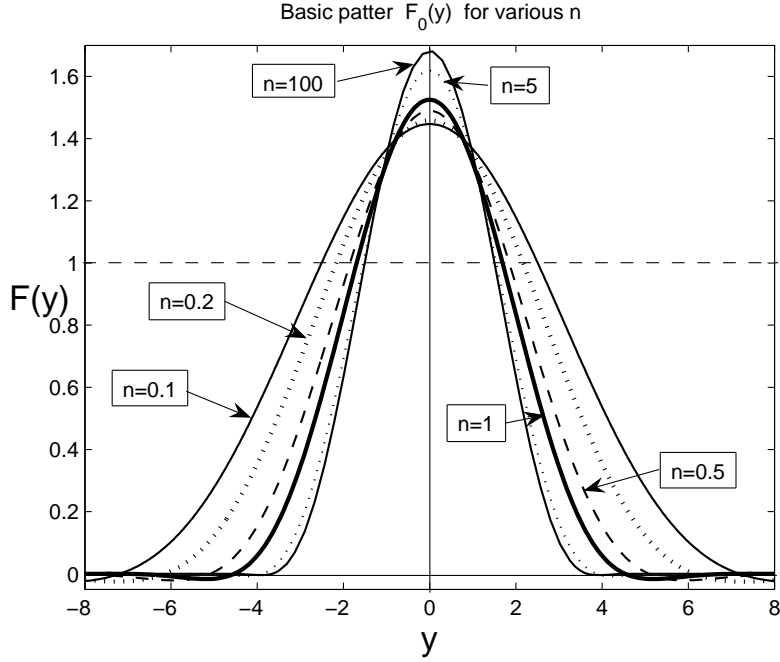


FIGURE 3. The first solution $F_0(y)$ of (5.2) for various n .

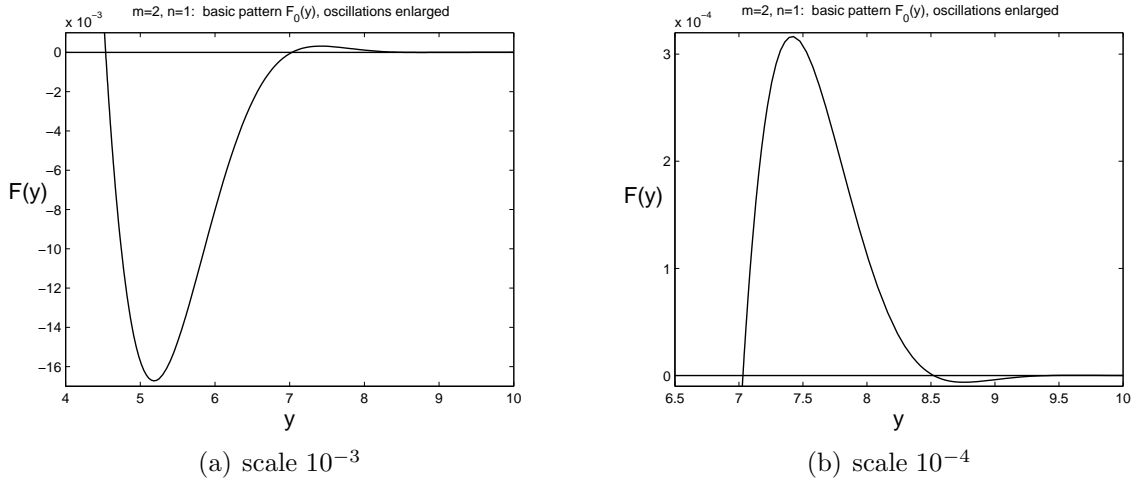


FIGURE 4. Enlarged zero structure of the profile $F_0(y)$ for $n = 1$ in the linear scale.

The behaviour (5.21) is then to be matched with the asymptotics near the interface at some $y = y_0^-(n) \gg 1$ (cf. (3.5)) that is governed by the non-Lipschitz term in (5.2),

$$(5.23) \quad F^{(4)} = -|F|^{-\frac{n}{n+1}} F + \dots \implies F(y) = (y_0 - y)^{\frac{4(n+1)}{n}} \varphi_*(\ln(y_0 - y)) + \dots,$$

where φ_* is the corresponding periodic solution of the ODE for the oscillatory component. A dimensional analysis implies that the interface position can be estimated as follows:

$$(5.24) \quad y_0(n) \sim n^{-\frac{3}{4}} \quad \text{as } n \rightarrow 0^+;$$

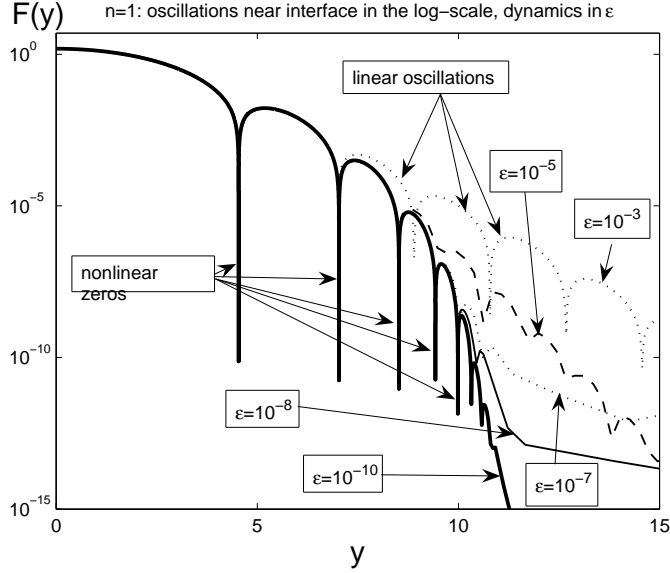


FIGURE 5. Behaviour of $F_0(y)$ for $n = 1$ in the log-scale near the interface: formation of five nonlinear zeros as $\varepsilon = \text{Tols}$ decrease from 10^{-3} to 10^{-7} .

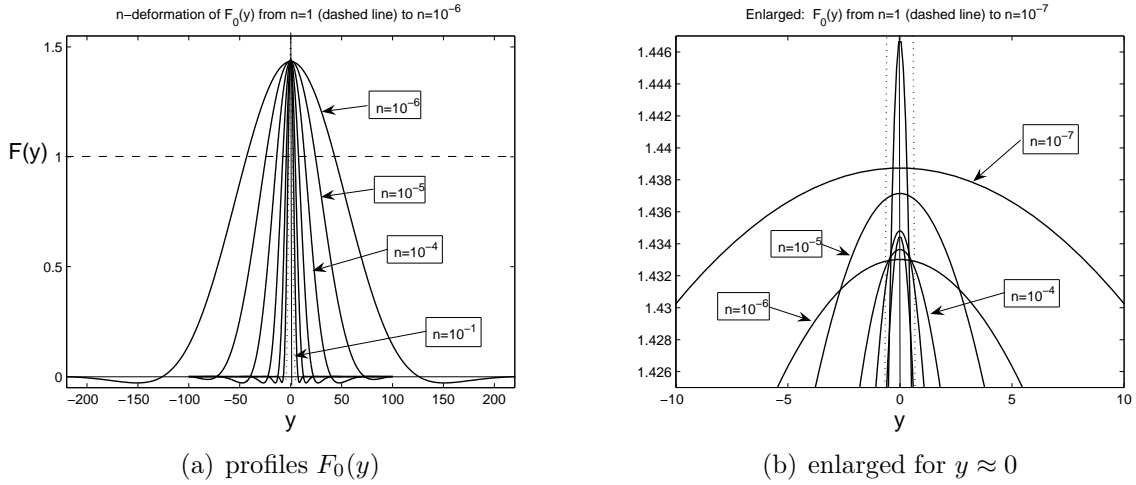


FIGURE 6. Deformation of the similarity solutions $F_0(y)$ of the ODE (5.2) for small $n > 0$.

see [16, § 9.6] for details. First rough matching of (5.21) and (5.23), (5.24) yields

$$A_0(n) \sim n^{\frac{3}{2}}.$$

A more accurate matching is difficult and typically assumes appearing logarithmic, $\ln n$, and other terms including oscillatory ones; see [16, § 7].

5.5. Basic countable family. Figure 7 shows¹ the basic family denoted by $\{F_l, l = 0, 1, 2, \dots\}$ of solutions of (5.2) for $n = 1$. This is associated with the application of L–S and fibering theory, [23]. Each profile $F_l(y)$ has $l + 1$ “dominant” extrema and l “transversal” zeros; see [23, § 5] and [22, § 4] for further details. We claim that

all the internal zeros of $F_l(y)$ are transversal

(excluding the oscillatory end points of the support), and this is a fundamental conclusion of our analysis, which deserves more rigorous treatment. In other words, each profile F_l is approximately obtained by a simple “interaction” (gluing together) of $l + 1$ copies of the first pattern $\pm F_0$ taking with necessary signs; see further comments below.

Actually, if we forget for a moment about the complicated oscillatory structure of solutions near interfaces, where an infinite number of extrema and zeros occur, the dominant geometry of profiles in Figure 7 approximately obeys Sturm’s classic zero set property, which is true rigorously for the second-order ODE only,

$$(5.25) \quad F'' = -F + |F|^{-\frac{n}{n+1}} F \quad \text{in } \mathbb{R}.$$

For (5.25), the basic family $\{F_l\}$ is constructed by direct gluing together simple patterns $\pm F_0$ given explicitly; see [25, p. 168]. Therefore, each F_l consists of $l + 1$ patterns (with signs $\pm F_0$), so that Sturm’s property is clearly true.

5.6. Countable family of $\{F_0, F_0\}$ -gluing and extensions. This procedure is similar to that in [21, § 4.7], but we again recall that these are completely different variational problems. Further patterns to be introduced do not exhibit as clear a “dominated” Sturm property and are associated with a double fibering technique where both Cartesian and spherical representations are involved; see details [23, § 6]. Let us present basic explanations.

The nonlinear interaction of the two first patterns $F_0(y)$ leads to a new family of profiles. In Figure 8 for $n = 1$, we show the first profiles from this family denoted by $\{F_{+2,k,+2}\}$, where in each function $F_{+2,k,+2}$ the multiindex $\sigma = \{+2, k, +2\}$ means, from left to right, $+2$ intersections with the equilibrium $+1$, then next k intersections with zero, and final $+2$ stands again for 2 intersections with $+1$. Later on, we will use such a multiindex notation to classify other patterns obtained.

Since $F_0(y)$ is infinitely oscillatory at the interfaces, the family $\{F_{+2,k,+2}\}$ is expected to be countable, so such functions exist for any even $k = 0, 2, 4, \dots$. Therefore, $k = +\infty$ leads to the non-interacting pair with no overlapping of supports,

$$(5.26) \quad F_0(y + y_0) + F_0(y - y_0), \quad \text{where } \text{supp } F_0(y) = [-y_0, y_0].$$

There exist various triple $\{F_0, F_0, F_0\}$ and any multiple interactions $\{F_0, \dots, F_0\}$ of arbitrarily large k single profiles, with a variety of distributions of zeros between any pair of neighbours.

¹Amazingly, these profiles look almost identical to those for the PDE (1.12) [21, § 4], corresponding to a completely different diffusion operator and much harder and distinct L–S theory. These similarities underline some quite obscure and involved common evolution properties of blow-up for different PDEs.

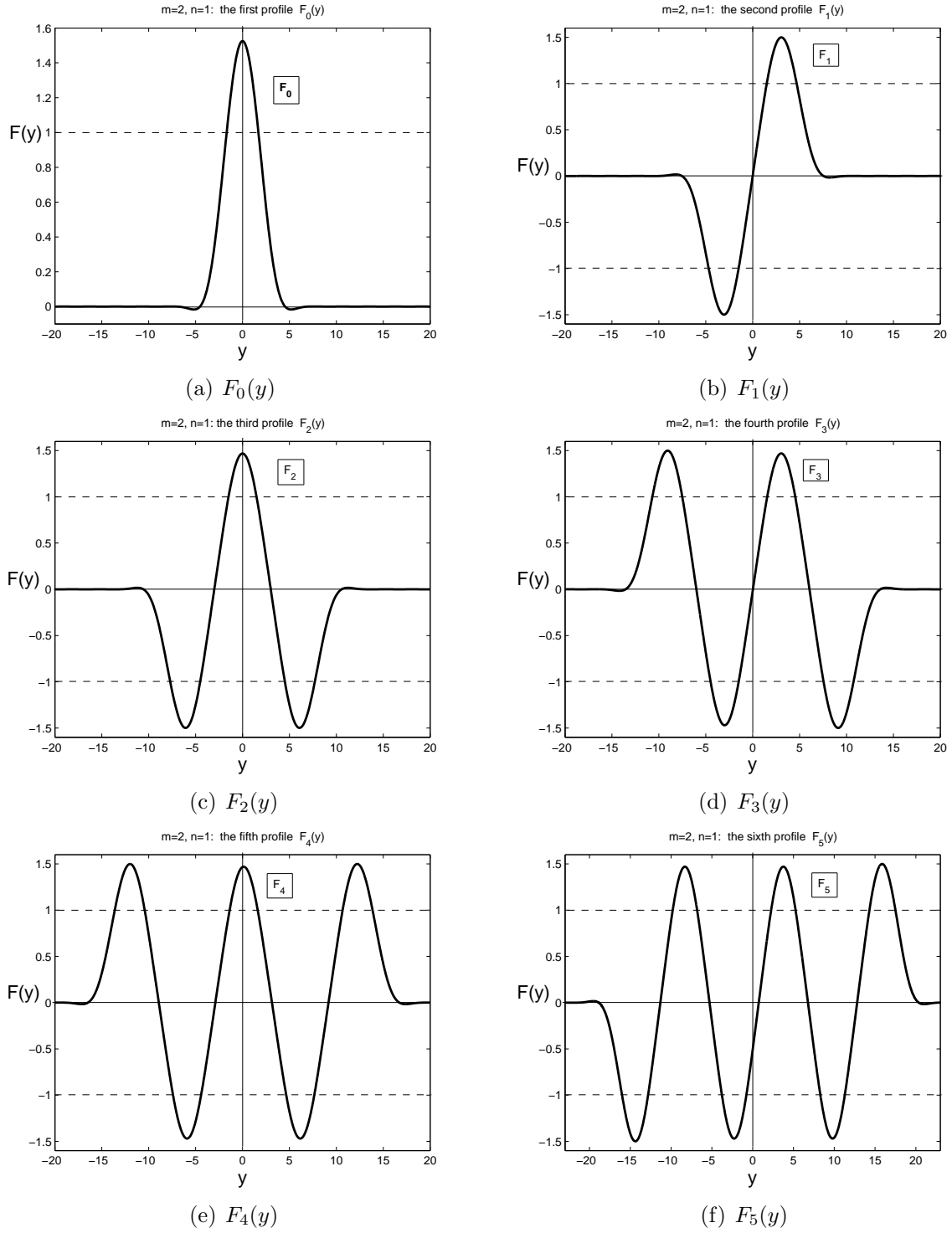


FIGURE 7. The first six patterns of the basic family $\{F_l\}$ of the ODE (5.2) for $n = 1$.

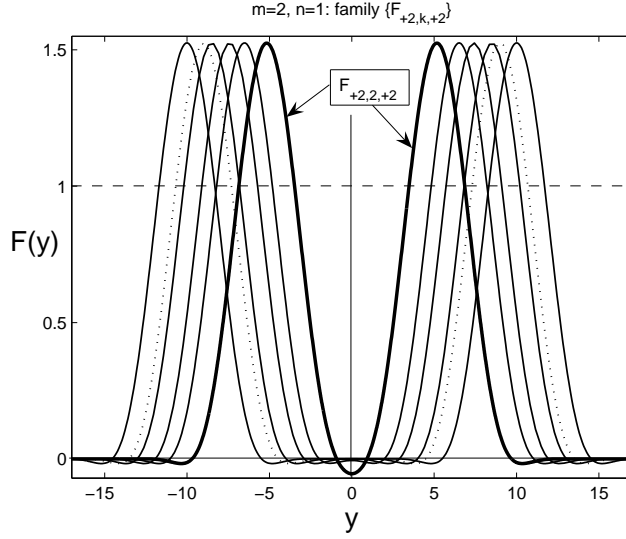


FIGURE 8. First patterns from the family $\{F_{+2,k,+2}\}$ of the $\{F_0, F_0\}$ -gluing; $n = 1$.

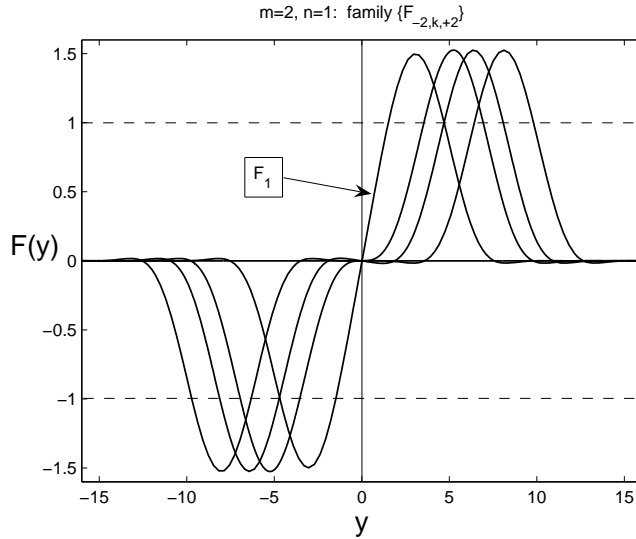


FIGURE 9. First four patterns from the family $\{F_{-2,k,+2}\}$ of the $\{-F_0, F_0\}$ -gluing; $n = 1$.

5.7. Countable family of $\{-F_0, F_0\}$ -gluing and extensions. Consider next the interaction of $-F_0(y)$ with $F_0(y)$. In Figure 9, for $n = 1$, we show the first profiles from this family denoted by $\{F_{-2,k,+2}\}$, where, for the multiindex $\sigma = \{-2, k, +2\}$, the first number -2 means 2 intersections with the equilibrium -1 , etc. The enlarged zero structure shows that the first two profiles belong to the same class $F_{-2,1,2}$, i.e., both have a single zero for $y \approx 0$. The last solution shown is $F_{-2,5,+2}$. This family $\{F_{-2,k,+2}\}$ is expected to be countable, with profiles existing for any odd $k = 1, 3, 5, \dots$, where the pair for $k = +\infty$ is non-interacting, $-F_0(y+y_0) + F_0(y-y_0)$. There can be constructed families of an arbitrary number of interactions such as $\{\pm F_0, \pm F_0, \dots, \pm F_0\}$ consisting of any $k \geq 2$ members.

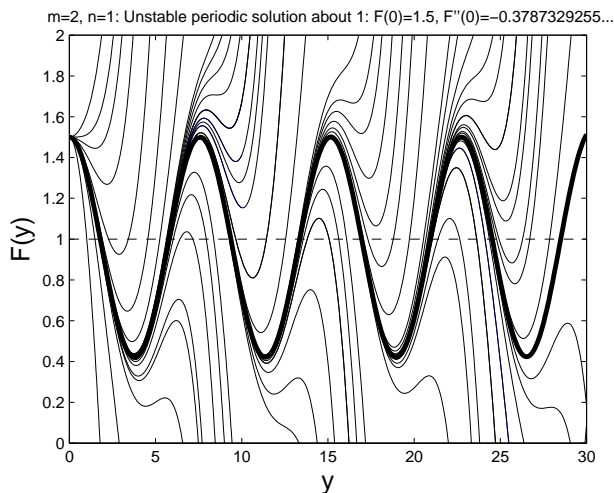


FIGURE 10. An example of a periodic solution of the ODE (5.2) for $n = 1$.

5.8. Periodic solutions in \mathbb{R} . We are going to introduce new types of patterns, which exhibit a different geometric shape. We then need first to describe non-compactly supported periodic solutions in \mathbb{R} . As a variational problem, equation (5.2) admits an infinite number of periodic solutions; see e.g. [34, Ch. 8]. Figure 10 for $n = 1$ presents a special unstable (as $y \rightarrow +\infty$) periodic solution obtained by shooting from the origin with conditions $F(0) = 1.5$, $F'(0) = F'''(0) = 0$, and $F''(0) = -0.3787329255\dots$. The periodic orbit $F_*(y)$ with the value

$$(5.27) \quad F_*(0) \approx 1.535\dots$$

will be shown to play a key role in the construction of other families of compactly supported patterns. Namely, this variety of solutions of (5.2) having oscillations about equilibria ± 1 are close to $\pm F_*(y)$ there.

5.9. Family $\{F_{+2k}\}$. The patterns F_{+2k} for $k \geq 1$ have $2k$ intersections with the single equilibrium $+1$ only and have a clear “almost” periodic structure of oscillations about it; see Figure 11(a). The number of intersections with $F = +1$ denoted by $+2k$ is an extra characterization of the Strum index to such a pattern. In this notation, $F_{+2} = F_0$.

5.10. Complicated and chaotic patterns. On the basis of our previous experience of dealing with various patterns, we will classify other solutions (possibly, a class of patterns) by introducing multiindices of any length

$$(5.28) \quad \sigma = \{\pm\sigma_1, \sigma_2, \pm\sigma_3, \sigma_4, \dots, \pm\sigma_l\}.$$

Figure 11(b) shows several profiles from the family with the index $\sigma = \{+k, l, -m, l, +k\}$. In Figure 12, we show further two different patterns, while in Figure 13, a single most complicated pattern is presented, for which

$$(5.29) \quad \sigma = \{-8, 1, +4, 1, -10, 1, +8, 1, 3, -2, 2, -8, 2, 2, -2\}.$$

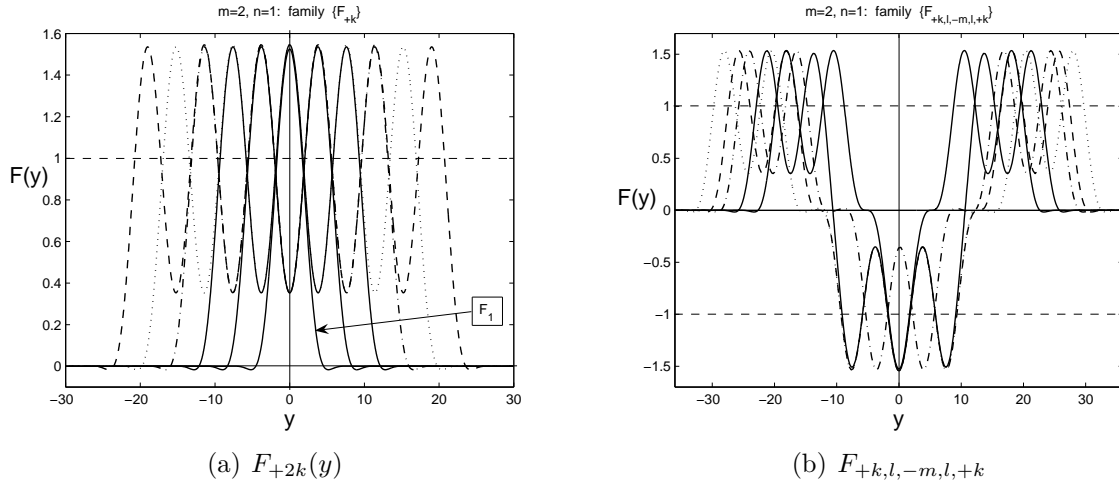


FIGURE 11. Two families of solutions of (5.2) for $n = 1$; $F_{+2k}(y)$ (a) and $F_{+k,l,-m,l,+k}$ (b).

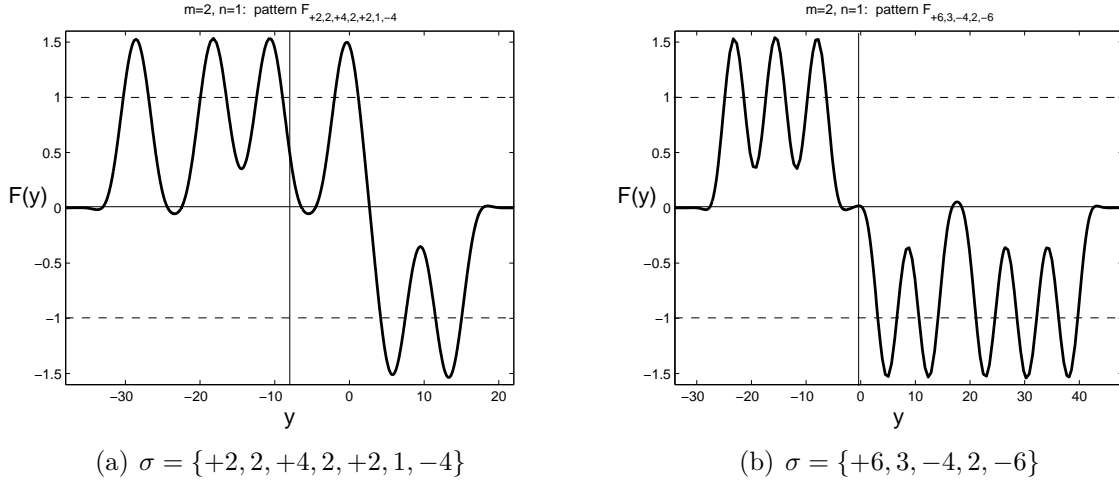


FIGURE 12. Two patterns for (5.2) for $n = 1$.

All computations are performed for $n = 1$ as usual, and numerics were well converged with sufficient accuracy and regularization at least $\sim 10^{-4} - 10^{-5}$ and better. This shows that the multiindex (5.28) can be arbitrary, i.e., can take any finite part of any non-periodic fraction. Though we do not insist that, for a given σ , the profile $F_\sigma(y)$ is unique, we have seen that the uniqueness fails. Note that the homotopy approach [30, 44] does not apply to ODEs such as (5.2) with infinite oscillatory properties.

Actually, this means *chaotic features* of the whole family of solutions $\{F_\sigma\}$. These chaotic types of behaviour are known for other fourth-order ODEs with coercive operators, [36, p. 198].

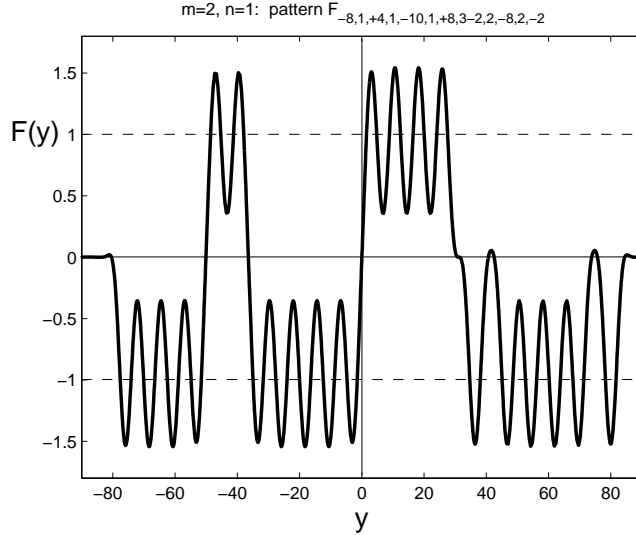


FIGURE 13. A complicated pattern $F_\sigma(y)$ for (5.2) for $n = 1$.

6. SINGLE POINT BLOW-UP FOR $p > n + 1$

We now consider the ODE (4.2) in the case $p > n + 1$, which, in view of the spatial rescaled variable y in (4.1), corresponds to single point blow-up. It is crucial that (4.2) for $p \neq n + 1$ is *not variational*. Therefore, the solutions of (4.2) can be traced out by a complicated shooting and matching procedures, which are still not completely justified. For practical reasons, we will use a continuation in parameters approach, which allows us to predict solutions by using those in the variational case $p = n + 1$. Recall that for such ODEs, using a standard inverse function theorem is not straightforward at all since the differential operator in (4.2) is degenerate and singular. Nevertheless, we will suggest to use Schauder's fixed point theorem and arrive at some convincing conclusions concerning the solvability and the multiplicity of solutions (the so-called p -branches of solutions).

6.1. Asymptotics at infinity and first numerical results. Recall that, according to our local analysis close to interfaces, such a behaviour for the TWs given by (3.3), (3.4) asymptotically coincides with that for the blow-up similarity solutions; cf. ODEs (5.2) and (5.23). We can continue to use this convenient analogy in the present case, since the ODE (4.2) provides us with similar asymptotics at the interfaces. Obviously, the behaviour at finite interface $y_0 > 0$ now corresponds to $\lambda = +1$, and therefore the *one-dimensional* bundle (3.13) is not sufficient to shoot two boundary conditions in (4.4) or (4.5). This explains why we need another asymptotic expansion as $y \rightarrow +\infty$. Thus, compactly supported similarity profiles are very unlikely (though may exist for some very special parameters values involved).

Thus, unlike the previous case of regional blow-up for $p = n + 1$, in the present case, in order to get a guaranteed successful shooting, we must use another full *two-dimensional* bundle of non-compactly supported solutions of (4.2) with the following behaviour:

$$(6.1) \quad f(y) \sim (C_0 y^\gamma + \dots) + (C_1 e^{-b_0 y^\nu} + \dots) \quad \text{as } y \rightarrow +\infty.$$

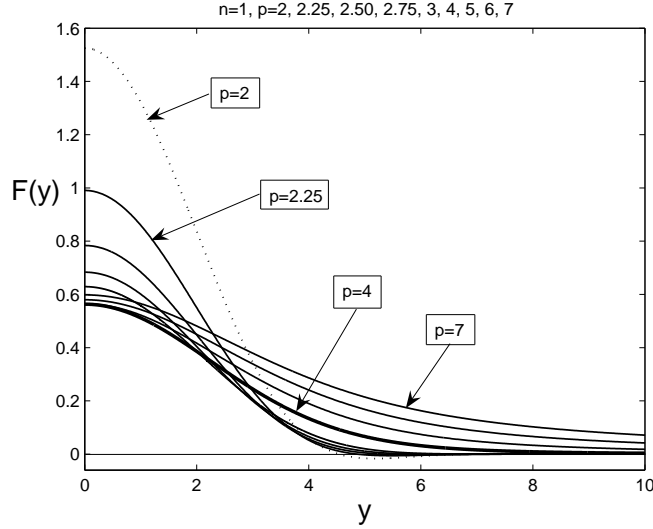


FIGURE 14. Single point blow-up patterns $F_0(y)$ of (4.2) for $n = 1$ and various $p \geq 2$.

Here $C_0 \neq 0$ and $C_1 \in \mathbb{R}$ are arbitrary constants and

$$\gamma = -\frac{4}{p-(n+1)} < 0, \quad \nu = \frac{4(p-1)}{3[p-(n+1)]} > 0, \quad b_0 = \frac{1}{\nu} \left(\frac{\beta}{n+1} C_0^{-n} \right)^{\frac{1}{3}} > 0.$$

Roughly speaking, the first bracket in (6.1) represents an “analytic” part of the expansion (e.g., for integer p , in terms of multiples of y^γ it can be represented as an analytic series; the proof of convergence is difficult), while the second braces gives the essentially “non-analytic” part. Such a structure in (6.1) is typical for saddle-node equilibria, [37, p. 311]. Of course, for the fourth-order ODE (4.2), this expansion does not admit a simple phase-plane interpretation (though the algebraic origin of the expansion is clear). Justification of (6.1) needs technical applications of fixed point theorems in weighted spaces of continuous functions defined for $y \gg 1$; see a typical example in [41, p. 29] and related references.

One can see passing to the limit $t \rightarrow T^-$ in (4.1) that the asymptotic behaviour (6.1) gives the following *final-time profile* of this single point blow-up for even profiles $f = f(|y|)$:

$$(6.2) \quad u_S(x, T^-) = C_0 |x|^{-\frac{4}{p-(n+1)}} < \infty \quad \text{for all } x \neq 0.$$

Returning to the asymptotic expansion, we conclude that (6.1) represents

$$(6.3) \quad \text{a 2D asymptotic bundle.}$$

Hence, the bundle (6.1) is well suitable for matching with also two symmetry conditions at the origin (4.4), so we expect not more than a countable set of solutions. For first patterns, we keep the same notation as in Section 5) for $p = n + 1$. Moreover, one can expect that these profiles can be continuously deformed to each other as $n \rightarrow 0^+$.

In Figure 14, we present the first pattern $F_0(y)$ for $n = 1$ with $p = 2$ (the dotted line for comparison), 2.25, 2.5, 2.75, 3, 4, 5, 6, 7. This shows that, for larger p , the profiles get the positive asymptotic behaviour (6.1) with $C_0 > 0$, and become strictly positive in \mathbb{R} .

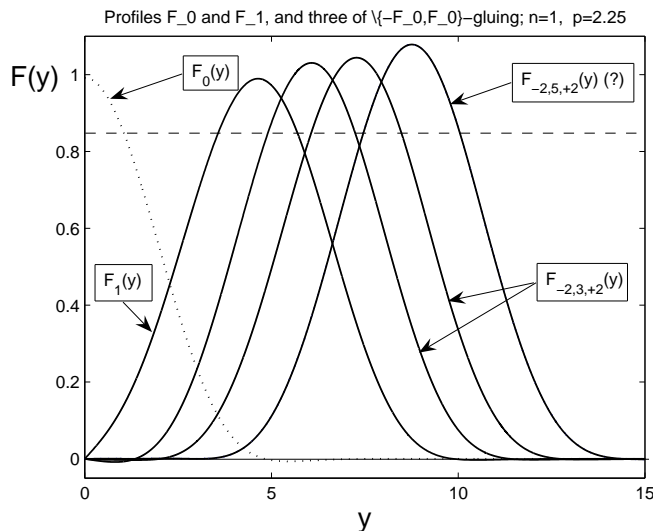


FIGURE 15. Single point blow-up patterns $F_0(y)$ and $F_1(y)$ of (4.2) and three profiles from the family $\{F_{-2,2k+1,+2}\}$ of the $\{-F_0, F_0\}$ -gluing; $n = 1$, $p = 2.25$.

Figure 15 shows the first $F_0(y)$ and the second $F_1(y)$ (dipole-like) patterns for $n = 1$ and $p = 2.25$. In addition, we show therein three profiles from the corresponding (possibly, finite for $p > n + 1$) family of $\{-F_0, F_0\}$ -gluing. This family can be viewed as the continuous p -extension of the family shown in Figure 9 in the variational case $p = n + 1$. Observe that we have two profiles $F_{-2,3,+2}(y)$, and in the last one $F_{-2,5,+2}(y)$ the structure of zeros close to $y = 0$ was not identified completely clear. Numerically, this is very difficult and convergence is very slow with the maximal number 20 000 of mesh points used in `bvp4c` solver with `Tols` $\sim 3 \cdot 10^{-3}$ achieved.

These numerics also confirm that the profiles have non-oscillatory asymptotic behaviour as in (6.1), though these can change sign a few (couple of) times, thus inheriting this finite oscillation property from the oscillatory one of the type (3.5) for $p = n + 1 = 2$ (sufficiently close to the current $p = 2.25$).

6.2. On branching of solutions from variational critical points: degree theory and Schauder's theorem. We again reduce (4.2) to the semilinear problem,

$$(6.4) \quad F = |f|^n f \implies -F^{(4)} - \beta(1 - \alpha)|F|^{-\alpha} F' y - \frac{1}{p-1} |F|^{-\alpha} F + |F|^{p(1-\alpha)-1} F = 0,$$

where $\alpha = \frac{n}{n+1}$. For $p = n + 1$, i.e., for $\beta = 0$, this ODE has been studied in Section 5. Setting $\varepsilon = p - (n + 1)$ and writing (6.4) as

$$(6.5) \quad \mathbf{G}(F) \equiv -F^{(4)} - \frac{1}{p-1} |F|^{-\alpha} F + |F|^{p(1-\alpha)-1} F = \varepsilon \frac{1-\alpha}{4(p-1)} |F|^{-\alpha} F' y,$$

we have that the non-autonomous term on the right-hand side becomes an asymptotically small perturbation for $|\varepsilon| \ll 1$ (in the “weak” integral sense for the equivalent integral equation, so the singularity $|F|^{-\alpha} F'$ is supposed to be eliminated via integration by parts; see (6.6)). On the other hand, the operator on the left is variational and hence the non-perturbed problem for $\varepsilon = 0$ admits families of solutions described in Section 5 (see more

details in [23]). Classic perturbation and branching theory [45, 31] suggests that, under natural hypotheses, the variational problem for $\varepsilon = 0$ can generate a countable family of p -branches, which can be extended for some sufficiently small $|\varepsilon| > 0$. The analysis of bifurcation, branching, and continuous extensions is then performed for the equivalent to (6.5) integral equations with Hammerstein compact operators; see typical examples in [9, 22, 29], where similar perturbation problems for blow-up and global patterns were investigated. Note that these p -branches of solutions are fully extensible and can end up either at a singularity point or at another bifurcation values.

Thus, for convenience, we write (6.5) as follows:

$$(6.6) \quad \begin{aligned} (\mathbf{B}^* - I)F &= h(F, \varepsilon) \equiv -\frac{1}{4}yF' + \varepsilon \frac{1-\alpha}{4(p-1)} |F|^{-\alpha} F'y + \frac{1}{p-1} |F|^{-\alpha} F \\ -|F|^{p(1-\alpha)-1}F &\implies F = \mathbf{A}(F, \varepsilon) \equiv (\mathbf{B}^* - I)^{-1}h(F, \varepsilon), \end{aligned}$$

where $(\mathbf{B}^* - I)^{-1}$ is a compact linear operator in $L^2_{p^*}(\mathbb{R})$, [13]. For $\varepsilon = 0$, (6.6) gives an integral equation with a variational operator, which admits the same critical values and points as the differential one studied before.

An efficient way to prove branching of solutions from $p = n + 1$, which applies for the lack of differentiability and regularity of nonlinearities involved, is using degree-index theory. This establishes branching from an isolated solution, say, the first one F_0 for simplicity, from the branching point $\varepsilon = 0$ provided its index (rotation of the vector field $I - \mathbf{A}'(F_0, 0)$) satisfies [31, p. 353]

$$(6.7) \quad \gamma = \text{ind}(F_0, I - \mathbf{A}'(F_0, 0)) \neq 0.$$

Unfortunately, for the equation (6.6), this approach hardly applies, since the operator contains nonlinearities $|F|^{-\alpha}F$, which are not differentiable at 0, so it is not completely clear how to treat the spectral properties of the self-adjoint operator $\mathbf{G}'(F_0)$ for setting in the whole space \mathbb{R} (not on a bounded interval corresponding to Dirichlet problems). Besides, the Fréchet differentiability of \mathbf{A} in F for $\varepsilon \neq 0$ is non-existent. Note that standard alternatives of bifurcation-branching theory without differentiability hypotheses assume sufficient regularity of the perturbations; cf. [11, Thm. 28.1]. Justification of branching phenomena in the present problem needs further deeper analysis and more tricky “functional topology” involved.

Continuing to describe spectral features of $\mathbf{G}'(F_0)$, we note that

$$\lambda = 0 \quad (\text{with the eigenfunction } \psi_0 \sim F'_0)$$

is an eigenvalue that corresponds to the translational invariance of the original PDE (1.8) with the infinitesimal generator D_y . Therefore, $\lambda = 1$ is an eigenvalue of $\mathbf{A}'(F_0, 0)$ (this derivative exists), and this leads the *critical case*, where computing of the index is more difficult and is performed as in [31, § 24]. It is more important that

$$\lambda = 1 \quad (\text{with the eigenfunction } \psi_1 \sim F_0)$$

is also an eigenvalue of $\mathbf{G}'(F_0)$ and this is associated with the generator D_t of the group of translations in t .

Thus, the index condition (6.7) needs special additional treatment, in particular, associated with spectral properties of the linearized operator $\mathbf{G}'(F)$, and this is an open problem. In this connection, we conjecture that $\varepsilon = 0$ is a *point of changing index* for the basic family $\{F_l\}$, and that [31, Thm. 56.2] applies to generate a countable set of continuous ε -curves from any basic pattern $F_l(y)$ constructed in Section 5.5.

Continuing branching approach, for non-differentiable nonlinearities as in (6.6), as an alternative (and less effective relative to branches detected) approach, we have that Schauder's Theorem can be applied to get solutions of (6.5) for small $\varepsilon > 0$ and to trace out p -branches of the suitable profiles. Let us be more precise about this extension of p -branches from the variational critical points at $p = n + 1$. Thus, we consider (6.6) as an integral equation in \mathbb{R} using the well-known spectral properties of the operator \mathbf{B}^* in Section 2 with compact resolvent; see [29, 22] for similar reductions. We then need to apply Schauder's fixed point Theorem [2, p. 90] in the framework of a weighted $L_{\rho^*}^p$ -metric, in which the integral Hammerstein-type operators involved are naturally compact; see [31, § 17]. One can see that the right-hand side in (6.6) is continuous in this topology at $\varepsilon = 0$, so that this gives at least one solution which is close to F_0 for $\varepsilon \approx 0$.

This somehow settles existence of at least one solution of (6.4) for small $|\varepsilon| > 0$ in a convex neighbourhood of solutions F_l for $p = n + 1$ (i.e., $\varepsilon = 0$). In this framework, uniqueness becomes a very difficult problem since the integral operators are not contractive in this metric. But we then obtain at least a single continuous p_l -branch emerging from $p = n + 1$. The global behaviour of p -branches is a hard problem to be tackled next.

6.3. Bifurcation from constant equilibria. Here we study other bifurcation phenomena in this problem: the p -bifurcation from the constant equilibrium $F(y) \equiv F_*$ for the ODE (6.4) (or (6.6)), where difficulties concerning non-differentiable nonlinearities do not occur. This leads to other non-basic profiles F . To this end, we use the known spectral properties of the adjoint operator (2.7). Set

$$(6.8) \quad F(y) = F_* + Y(y), \quad \text{where} \quad F_* = f_*^{n+1}$$

(i.e., $\pm F_*$ are equilibria for (6.4)), and write down (6.4) in the following form:

$$(6.9) \quad -Y^{(4)} - \beta(1 - \alpha)|F_*|^{-\alpha}Y'y - \frac{1}{p-1}(1 - \alpha)|F_*|^{-\alpha}Y + G(y, Y, Y') = 0,$$

where $G(\cdot)$ is the nonlinear part of the operator to be treated as a perturbation in the space $L_{\rho^*}^2$. We next set

$$(6.10) \quad y = az, \quad \text{where} \quad a^4\beta(1 - \alpha)|F_*|^{-\alpha} = \frac{1}{4}.$$

Then (6.9) reduces to

$$(6.11) \quad \mathbf{B}^*Y \equiv -Y^{(4)} - \frac{1}{4}Y'y = \frac{1}{p-(n+1)}Y - a^4G(z, Y, Y').$$

We finally apply classic bifurcation-branching theory [31, 45] for the equivalent integral operator with compact operators in $L_{\rho^*}^2(\mathbb{R})$ constructed similar to (6.6); see also extra

details in [28, 9, 22]. It follows from the linearized operator in (6.11) that bifurcation in p can occur at the following points:

$$(6.12) \quad \frac{1}{p-(n+1)} \in \sigma(\mathbf{B}^*) = \left\{ -\frac{l}{4} \right\} \implies p = p_l = n + 1 - \frac{4}{l} \quad \left(l > \frac{4}{n} \right).$$

Recall that all the eigenvalues $\lambda_l = -\frac{l}{4}$ of \mathbf{B}^* are simple, and hence, under typical assumptions, correspond to bifurcation points; see e.g., [11, p. 381]. The rigorous justification in the framework of functional setting in weighted $L^2_{\rho^*}$ -spaces and, especially, asymptotic expansions as $\varepsilon = p - p_l \rightarrow 0$ become rather tricky and involved; we do not do this here and we refer to typical examples in [9, § 5]. This creates a countable set of p -bifurcation branches to be described next. The adjoint polynomials $\psi_l^*(y)$ do not change sign (see (2.8)), so that the patterns obtained for $p \approx p_l^+$ are expected to have a minimal number (sometimes, none) of intersections with the constant equilibrium F_* . We do not know for sure how to classify these patterns and expect that as $p \rightarrow n + 1$ they are converted into the non-basic profiles F_{+2k} from Section 5.9 with large $k = k(l) > \frac{4}{n}$ (an open problem).

Thus, in general, there exists a countable family of p -branches, and some of them, being extended to $p = 1^-$, $n = 0$, are expected, after necessary scaling, to match with the countable set of linear profiles given in (4.8); cf. [29, § 6.1]. A reliable rigorous identification of these p -branches for the integral equation of the type (6.6) is a difficult analytical, as well as numerical problem.

Since (6.12) makes no sense for $l = 0$ (and other small l 's), classic bifurcation theory [11, p. 401] suggests that the basic p_0 -branch of $F_0(y)$ of the simplest shape (as well as other first ones with $l \leq \frac{4}{n}$) is assumed to exist for all $p > 1$. In other words, this branch cannot appear at bifurcation points such as those indicated in (6.12). In Figure 16, we show the first p -branch of F_0 (a) and the deformation of the profiles $F_0(y)$, (b). We expect that this p_0 branch is composed from stable solutions and hence represents the generic asymptotic blow-up behaviour for the parabolic PDE (1.8).

A small part of the next p_1 -branch of dipole-like profiles $F_1(y)$ for $n = 1$ and $p \in [2, 2.11]$ is shown in Figure 17(a), where (b) demonstrates the corresponding deformation with p of $F_1(y)$. Further extension of this branch beyond $p = 2.17$ leads to strong instabilities where the profiles suddenly jump to different shapes (which possibly belong to other p -branches nearby having the geometric structure as in Figure 9; we did not construct such neighbouring branches).

The p -branches can connect various profiles, with rather obscure understanding of possible geometry of such branches and their saddle-node bifurcations (turning) points. For $p = n + 1$, the questions on connections with respect to regularization parameters are addressed in [23, § 7] posing problems of homotopy classification of patterns in variational problems and approximate ‘‘Sturm index’’ of solutions.

For instance, Figure 18 for $n = 1$ shows the connection of the profile $F_1(y)$ for $p = 2.2$ (cf. the previous figure) with two ‘‘almost independent’’ mutually shifted profiles $\pm F_0$ for $p = 2$. Next Figure 19, in the enlarged form, explains formation of the zero set of profiles and shows in (b) that the eventual structure for $p = 2$ actually belongs for a member of the

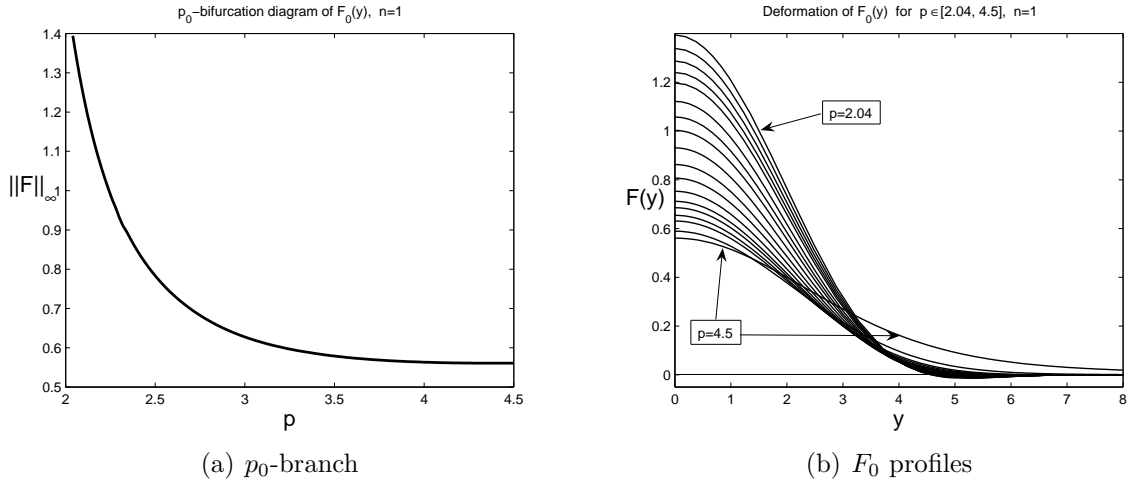


FIGURE 16. The first p_0 -branch of solutions $F_0(y)$ of equation (6.4) for $n = 1$ (a); corresponding deformation of F_0 (b).

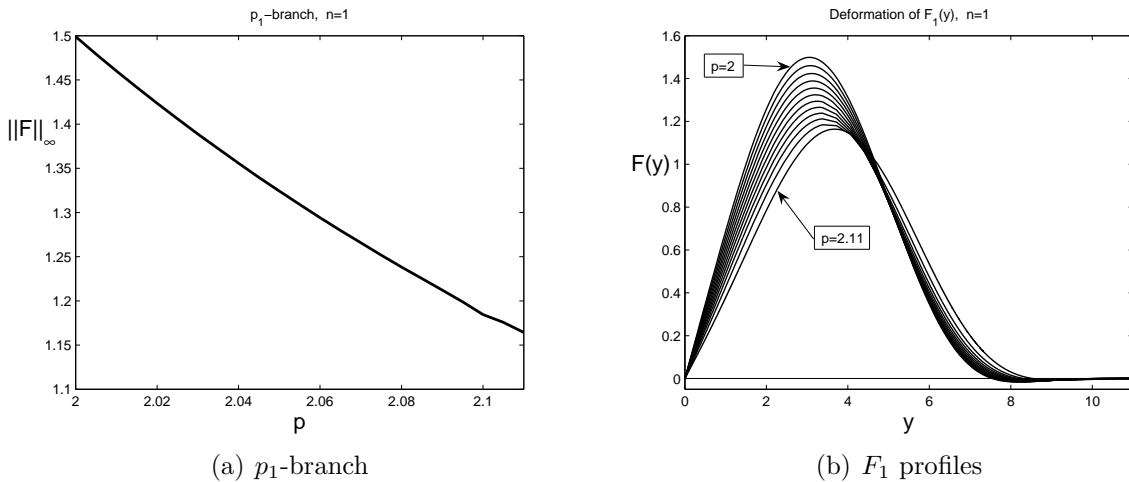


FIGURE 17. The second p_1 -branch of solutions $F_1(y)$ of equation (6.4) for $n = 1$ (a); corresponding deformation of F_1 (b).

family $\{-F_0, F_0\}$ -gluing, i.e., it is the profile $F_{-2,7,+2}(y)$, with exactly seven transversal zeros between $\pm F_0(y)$ structures.

The principle fact that higher-order p -branches of the basic family $\{F_l\}$ (see Section 5.5) can be originated from $p = n + 1$ is illustrated in Figure 20 where we show the p_2 -branch of profiles $F_2(y)$ (a) (for $p = n + 1$, this profiles is given in Figure 7(c)) and the deformation of the profiles (b).

Another principal issue is justified in Figure 21 that shows the p -branch of the profile $F_{+2,2,+2}(y)$; cf. Figure 8 for $p = n + 1$.

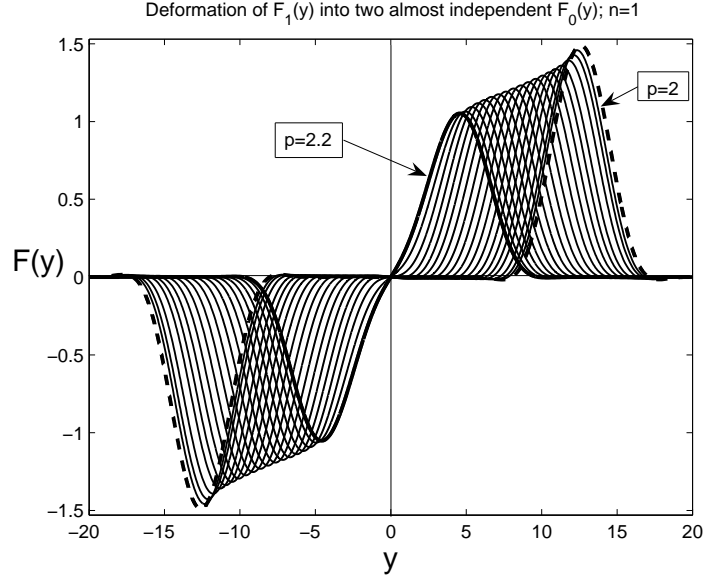


FIGURE 18. Deformation of $F_1(y)$ for $p \in [2, 2.2]$; $n = 1$.

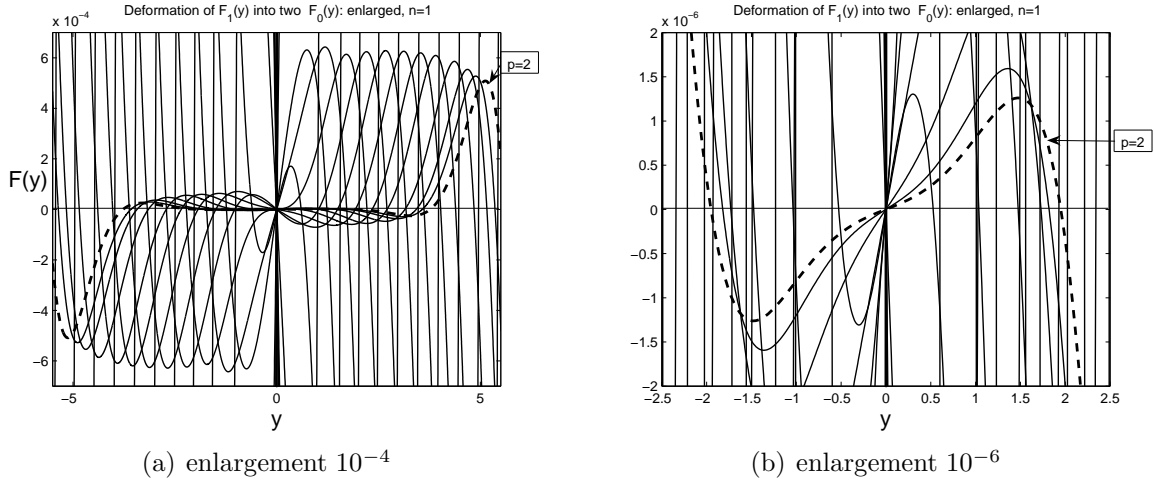


FIGURE 19. Enlarged zero set for profiles in Figure 18; (b) shows that for $p = 2$, it is $F_{+2,7,-2}(y)$.

Concerning other, more complicated profiles for $p = n + 1$, such as $F_{+4}(y)$ and others containing such structures shown in Figures 8 and 12, numerical results suggest that these cannot be extended for $p > n + 1$. For instance, Figure 22 demonstrates that the profile $F_{+4}(y)$ very quickly jumps to the type $F_{+2,2,+2}$ (cf. Figure 21) for the increment $\Delta p = 10^{-3}$, and even for smaller Δp 's. This illustrates the fact that both profiles are very close and are originated at the same branching point. We do not intend here to get numerically a correct bifurcation diagram for this delicate case. It seems that this demands more

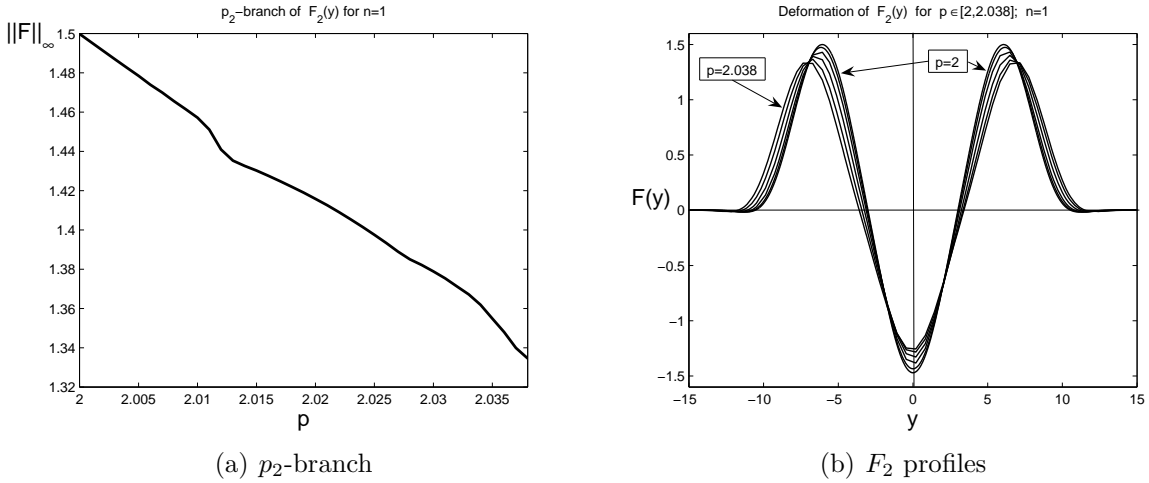


FIGURE 20. The third p_2 -branch of solutions $F_2 \equiv F_{+2,1,-2,1,+2}$ of equation (6.4) for $n = 1$ (a); corresponding deformation of F_2 (b).

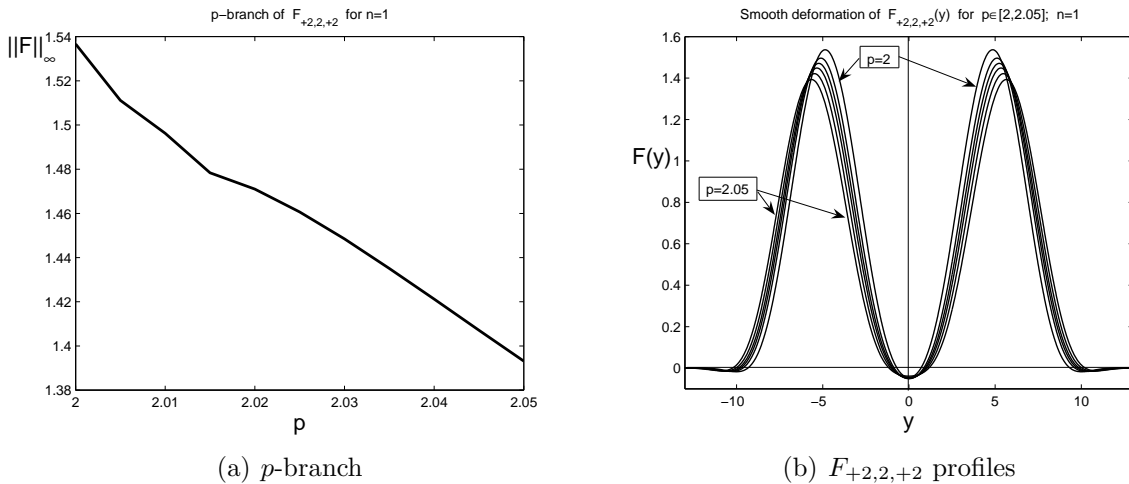


FIGURE 21. The p -branch of solutions $F_{+2,2,+2}$ of equation (6.4) for $n = 1$ (a); corresponding deformation of $F_{+2,2,+2}$ (b).

advanced parameter continuation techniques that are available in the standard `MatLab` environment. See a similar unstable case below for $p < n + 1$.

Remark: on μ -bifurcations. The origin of various branches of solutions can be also seen via an additional parameterization; cf. [9, § 4.3]. Namely, we consider equation (6.9), where we introduce the parameter by replacing

$$\beta \mapsto \mu > 0.$$

Then, linearizing as above, we conclude that bifurcation points are (for even profiles)

$$(6.13) \quad \mu_l = \frac{1}{l}, \quad l = 2, 4, \dots$$

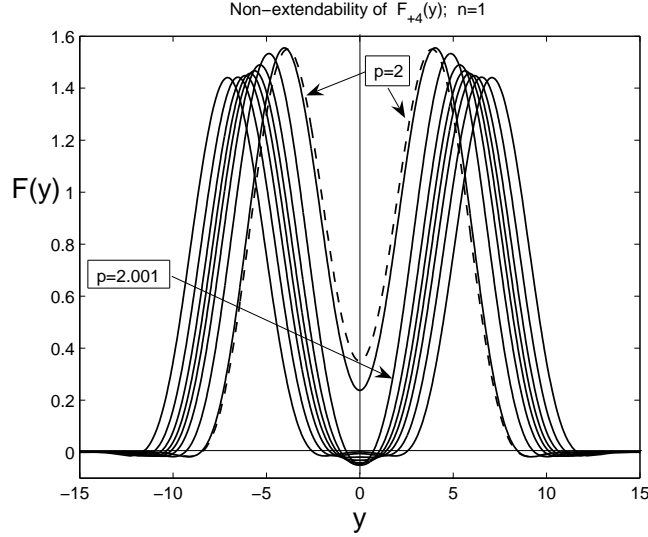


FIGURE 22. F_{+4} for $p = n + 1$ jumps to $F_{+2,2,+2}$ if p is increased by 10^{-3} ; $n = 1$.

Since $\beta < \frac{1}{4} < \frac{1}{2}$, we have that at least two bifurcation branches originated at μ_2 and μ_4 , we have a good chance to be extended to $\mu = \beta$ (this global continuation is an open mathematical problem, but can be checked numerically), and hence generate solutions of the original ODE (4.2).

7. GLOBAL BLOW-UP SIMILARITY PROFILES FOR $p \in (1, n + 1)$

For $p \in (1, n + 1)$, we have $\beta < 0$ in (4.1), so that the similarity solutions describe expanding as $t \rightarrow T^-$ waves with global blow-up uniformly on any compact subset in x .

7.1. Same oscillatory behaviour close to interfaces. The ODE (4.2) reads for $f \approx 0$

$$-(|f|^n f)^{(4)} - \beta y f' + \dots = 0 \quad (\beta < 0),$$

so, replacing $y_0 - y \mapsto y$, on integration for $y \approx 0$, we have

$$(|f|^n f)''' = +\beta y_0 f + \dots$$

This gives (3.3), where $\lambda = \beta y_0 < 0$ is reduced to -1 by scaling. Thus, for $p \in (1, n + 1)$, the similarity profiles are oscillatory near interfaces as for $p = n + 1$. By (3.7), the 2D asymptotic bundle is enough to match two symmetry boundary conditions (4.4), and the proof of matching remains open.

7.2. Profiles and branches. It turns out that, for $1 < p < n + 1$, the ODE (6.4) is more difficult to solve numerically than for $p \geq n + 1$. In Figure 23, for $n = 1$, we present the p_0 -branch of the generic profiles F_0 by continuation in p from $p = 2.5$ (single point blow-up) until $p = 1.7 < n + 1 = 2$ (global blow-up). The actual continuous p -deformation of functions $F_0(y)$ is seen from Figure 24. For smaller $p > 1$, the similarity profiles $F_0(y)$ become larger (and according to (4.3) the corresponding constant equilibria diverge

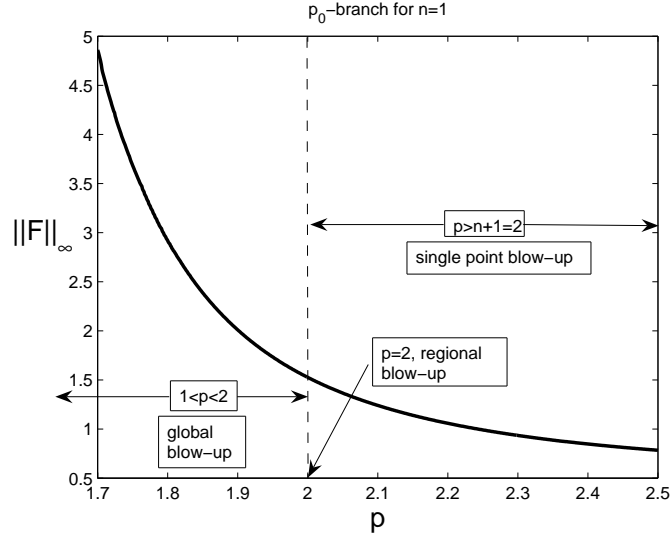


FIGURE 23. The p_0 -branch of $F_0(y)$ of the ODE (6.4) for $n = 1$.

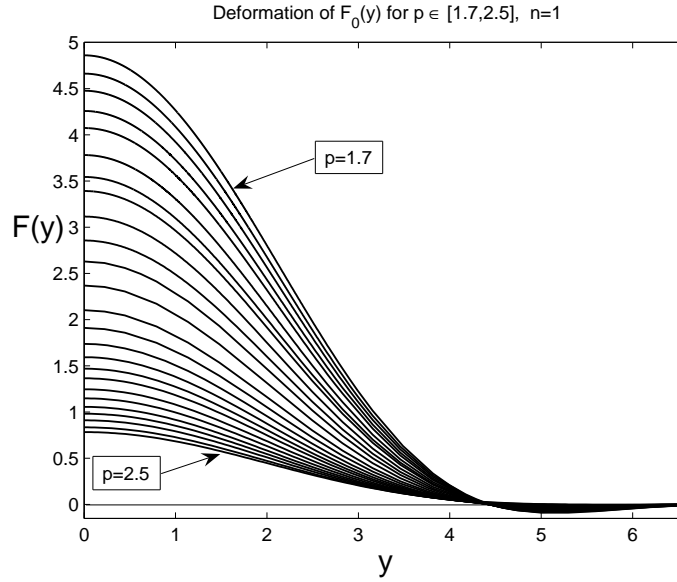


FIGURE 24. Deformation of $F_0(y)$ from Figure 23.

exponentially as $p \rightarrow 1^-$) and more oscillatory close to the interface. Note that the p_0 -branch is expected to consist of asymptotically (structurally) stable blow-up profiles $F_0(y)$, but we cannot prove this even in the linearized approximation (the linearized operator is a difficult non-self-adjoint operator with unknown spectrum).

In order to avoid the exponential discrepancy (4.3) of branches as $p \rightarrow 1^-$, we now perform in the ODE (6.4) the following additional scaling:

$$(7.1) \quad F \mapsto CF, \quad y \mapsto ay, \quad C^{(1-\alpha)(p-1)} = \frac{1}{p-1}, \quad a^4 = C^{-(1-\alpha)(p-1)} \quad (C = F_*^{\frac{1}{1-\alpha}})$$

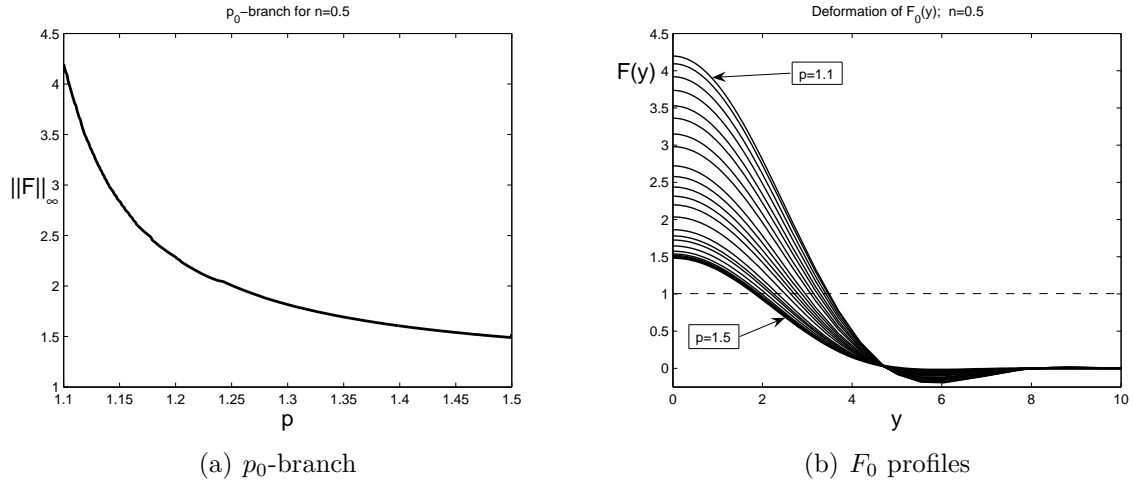


FIGURE 25. The p -branch of solutions $F_0(y)$ of equation (7.2) for $n = 0.5$ (a); corresponding deformation of $F_{+2,2,+2}$ (b).

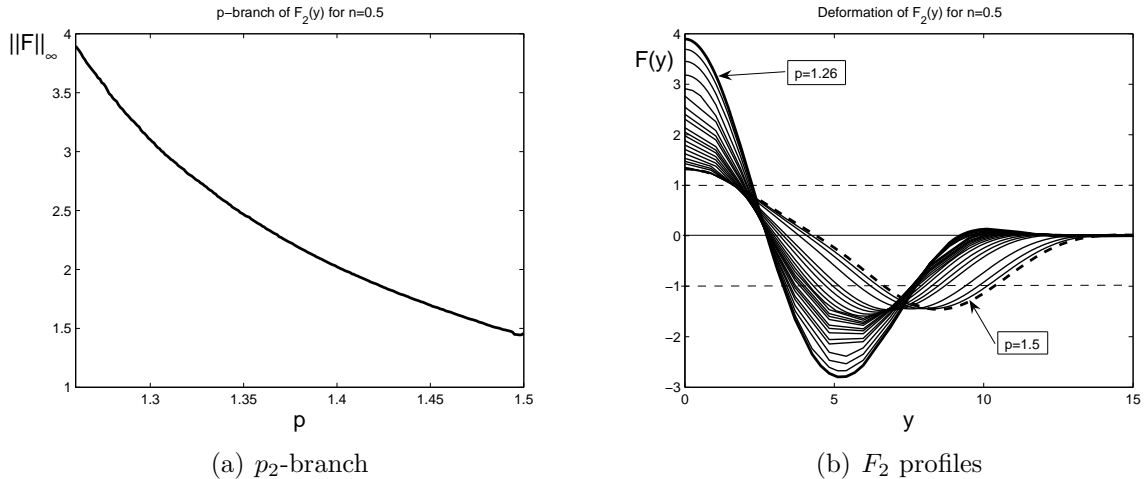


FIGURE 26. The p -branch of solutions $F_2(y)$ of equation (7.2) for $n = 0.5$ (a); corresponding deformation of $F_{+2,2,+2}$ (b).

to get the equation with fixed equilibria $F_* = \pm 1$ and 0:

$$(7.2) \quad -F^{(4)} - \beta(p-1)(1-\alpha)|F|^{-\alpha}F'y - |F|^{-\alpha}F + |F|^{p(1-\alpha)-1}F = 0 \quad \left(\alpha = \frac{n}{n+1}\right).$$

In Figure 25, we show the p_0 -branch for the ODE (7.2) with $n = 0.5$ and $p \in [1.1, 1.5]$. In Figure 26, we show the p_2 -branch of the profiles $F_2(y) \equiv F_{-2,1,+2,1,-2}(y)$ for the ODE (7.2) with $n = 0.5$ (a small “discontinuity” is seen there).

Concerning more complicated profiles not from the basic family $\{F_l\}$, in Figures 27 and 28, we show the p -branches of the profiles $F_{+4}(y)$ and $F_{+2,2,+2}(y)$ for the ODE (7.2) with $n = 0.5$. We observe that both p -branches (and the corresponding deformations) look

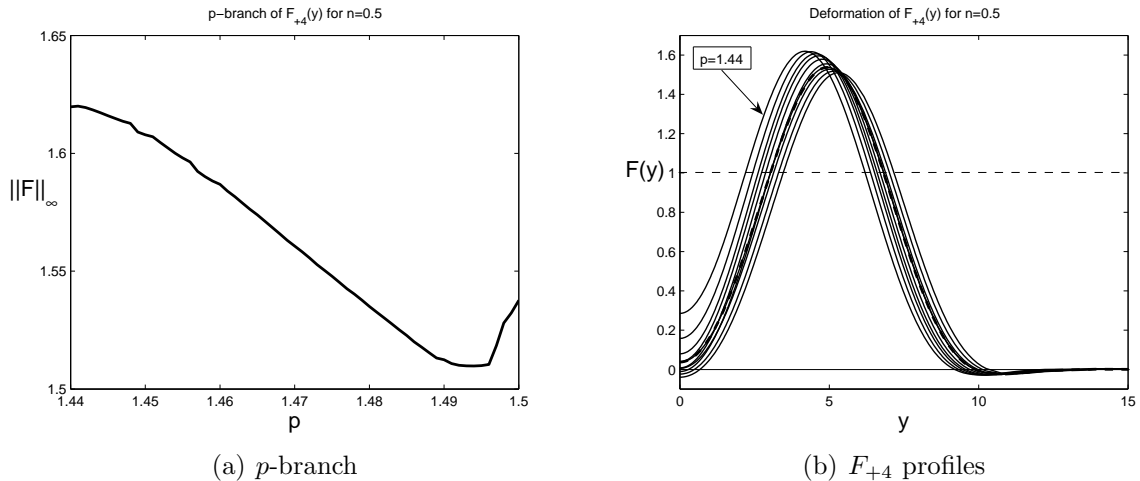


FIGURE 27. The p -branch of solutions $F_{+4}(y)$ of equation (7.2) for $n = 0.5$ (a); corresponding deformation of F_{+4} (b).

very similar, and actually, they do coincide for

$$p \leq p_* \approx 1.487.$$

We then claim that there exists a *branching point* $p = p_* \in (1, n + 1)$, at which the p -branch splits into two, thus giving us two different profiles with similar geometric shapes; see [45] for classic branching theory. Then this is not a standard saddle-node bifurcation, and analytical (and numerical) justification of such branching for the equivalent integral equation with non-differentiable nonlinearities represents a difficult open problem. Note that, according to (6.12), higher-order profiles F_{+2k} and geometrically neighbouring ones $F_{+2,2,\dots,+2}$ can also appear at bifurcations from the constant equilibrium F_* . This needs special research and remains an open problem.

Finally, we must admit that our numerics did not detect the p -extensions to the global blow-up range $p < n + 1$ of the odd (anti-symmetric) basic profiles such as $F_1(y)$ ((b) in Figure 7), or $F_3(y)$ ((d) in Figure 7). We always observed a strong divergence of the method applied to the ODE (7.2) without obvious reasons. Nevertheless, we expect that these p -branches of basic blow-up profiles do exist. This formal conclusion is associated with the question of evolution completeness of blow-up solutions for the PDE (1.8): indeed, then which patterns will describe a generic evolution as $t \rightarrow T^-$ for classes of anti-symmetric initial data? Of course, these could be non-similarity solutions, but those hard questions are definitely out of the present rather preliminary self-similar consideration.

Acknowledgement. The author would like to thank both the anonymous Reviewers for careful reading the manuscript and a number of useful suggestions that have been used in the final version.

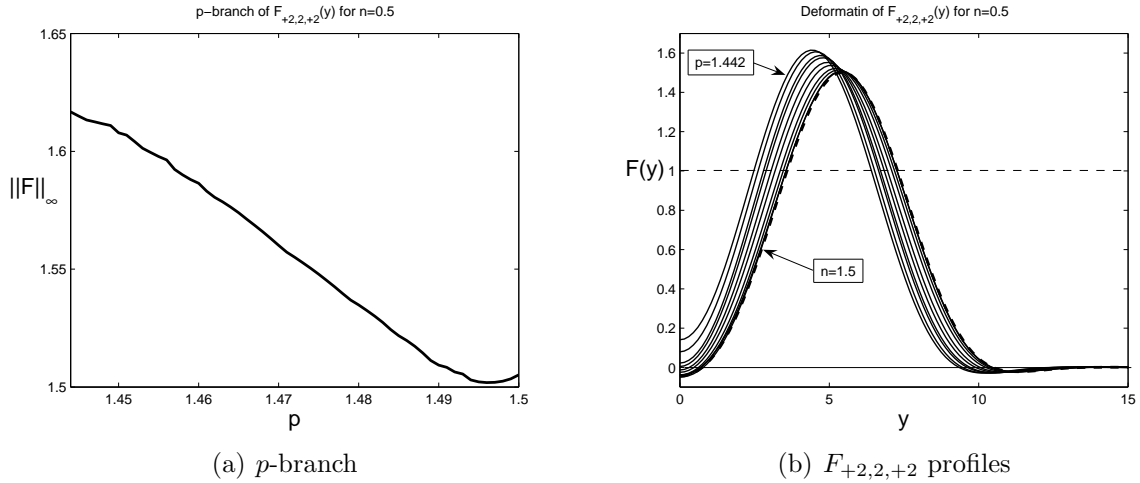


FIGURE 28. The p -branch of solutions $F_{+2,2,+2}(y)$ of equation (7.2) for $n = 0.5$ (a); corresponding deformation of $F_{+2,2,+2}$ (b).

REFERENCES

- [1] J. Bebernes and D. Eberly, *Mathematical Problems in Combustion Theory*, Appl. Math. Sci., Vol. **83**, Springer-Verlag, Berlin, 1989.
- [2] M. Berger, *Nonlinearity and Functional Analysis*, Acad. Press, New York, 1977.
- [3] F. Bernis, *Finite speed of propagation and asymptotic rates for some nonlinear higher order parabolic equations with absorption*, Proc. Roy. Soc. Edinburgh, **104A** (1986), 1–19.
- [4] F. Bernis, *Source-type solutions of fourth order degenerate parabolic equations*, In: Proc. Microprogram Nonlinear Diffusion Eqs Equilibrium States, W.-M. Ni, L.A. Peletier, and J. Serrin, Eds., MSRI Publ., Berkeley, California, Vol. 1, New York, 1988, pp. 123–146.
- [5] F. Bernis and A. Friedman, *Higher order nonlinear degenerate parabolic equations*, J. Differ. Equat., **83** (1990), 179–206.
- [6] F. Bernis and J.B. McLeod, *Similarity solutions of a higher order nonlinear diffusion equation*, Nonl. Anal., TMA, **17** (1991), 1039–1068.
- [7] A.L. Bertozzi and M.C. Pugh, *Long-wave instabilities and saturation in thin film equations*, Comm. Pure Appl. Math., **LI** (1998), 625–651.
- [8] A.L. Bertozzi and M.C. Pugh, *Finite-time blow-up of solutions of some long-wave unstable thin film equations*, Indiana Univ. Math. J., **49** (2000), 1323–1366.
- [9] C.J. Budd, V.A. Galaktionov, and J.F. Williams, *Self-similar blow-up in higher-order semilinear parabolic equations*, SIAM J. Appl. Math., **64** (2004), 1775–1809.
- [10] M. Chaves and V.A. Galaktionov, *Regional blow-up for a higher-order semilinear heat equations*, Euro J. Appl. Math., **12** (2001), 601–623.
- [11] K. Deimling, *Nonlinear Functional Analysis*, Springer-Verlag, Berlin/Tokyo, 1985.
- [12] Yu.V. Egorov, V.A. Galaktionov, V.A. Kondratiev, and S.I. Pohozaev, *On the necessary conditions of existence to a quasilinear inequality in the half-space*, Comptes Rendus Acad. Sci. Paris, Série I, **330** (2000), 93–98.
- [13] Yu.V. Egorov, V.A. Galaktionov, V.A. Kondratiev, and S.I. Pohozaev, *Asymptotic behaviour of global solutions to higher-order semilinear parabolic equations in the supercritical range*, Adv. Differ. Equat., **9** (2004), 1009–1038.
- [14] S.D. Eidelman, *Parabolic Systems*, North-Holland Publ. Comp., Amsterdam/London, 1969.

- [15] J.D. Evans, V.A. Galaktionov, and J.R. King, *Blow-up similarity solutions of the fourth-order unstable thin film equation*, Euro J. Appl. Math., **18** (2007), 195–231.
- [16] J.D. Evans, V.A. Galaktionov, and J.R. King, *Source-type solutions of the fourth-order unstable thin film equation*, Euro J. Appl. Math., **18** (2007), 273–321.
- [17] V.A. Galaktionov, *On conditions for there to be no global solutions of a class of quasilinear parabolic equations*, USSR Comput. Math. and Math. Phys., **22** (1982), 73–90.
- [18] V.A. Galaktionov, *On a spectrum of blow-up patterns for a higher-order semilinear parabolic equations*, Proc. Royal Soc. London A, **457** (2001), 1–21.
- [19] V.A. Galaktionov, *Geometric Sturmian Theory of Nonlinear Parabolic Equations and Applications*, Chapman and Hall/CRC, Boca Raton, Florida, 2004.
- [20] V.A. Galaktionov, *On interfaces and oscillatory solutions of higher-order semilinear parabolic equations with nonlipschitz nonlinearities*, Stud. Appl. Math., **117** (2006), 353–389.
- [21] V.A. Galaktionov, *Three types of self-similar blow-up for the fourth-order p -Laplacian equation with source*, J. Comp. Appl. Math. (2008), doi:10.1016/j.cam.2008.01.027.
- [22] V.A. Galaktionov and P.J. Harwin, *Non-uniqueness and global similarity solutions for a higher-order semilinear parabolic equation*, Nonlinearity, **18** (2005), 717–746.
- [23] V.A. Galaktionov and S.I. Pohozaev, *Refined complicated structure of similarity solutions of higher-order parabolic, hyperbolic, and nonlinear dispersion PDEs: an analytic-numerical approach*, Proc. Russian Acad. Sci., to appear.
- [24] V.A. Galaktionov and A.E. Shishkov, *Saint-Venant’s principle in blow-up for higher-order quasilinear parabolic equations*, Proc. Royal Soc. Edinburgh, Sect. A, **133A** (2003), 1075–1119.
- [25] V.A. Galaktionov and S.R. Svirshchevskii, *Exact Solutions and Invariant Subspaces of Nonlinear Partial Differential Equations in Mechanics and Physics*, Chapman & Hall/CRC, Boca Raton, Florida, 2007.
- [26] V.A. Galaktionov and J.L. Vazquez, *The problem of blow-up in nonlinear parabolic equations*, Discr. Cont. Dyn. Syst., **8** (2002), 399–433.
- [27] V.A. Galaktionov and J.L. Vazquez, *A Stability Technique for Evolution Partial Differential Equations. A Dynamical Systems Approach*, Progr. in Nonl. Differ. Equat. and Their Appl., Vol. **56**, Birkhäuser, Boston/Berlin, 2004.
- [28] V.A. Galaktionov and J.F. Williams, *Blow-up in a fourth-order semilinear parabolic equation from explosion-convection theory*, Euro. J. Appl. Math. **14** (2003), 745–764.
- [29] V.A. Galaktionov and J.F. Williams, *On very singular similarity solutions of a higher-order semilinear parabolic equation*, Nonlinearity, **17** (2004), 1075–1099.
- [30] W.D. Kalies, J. Kwapisz, J.B. VandenBerg, and R.C.A.M. VanderVorst, *Homotopy classes for stable periodic and chaotic patterns in fourth-order Hamiltonian systems*, Commun. Math. Phys., **214** (2000), 573–592.
- [31] M.A. Krasnosel’skii and P.P. Zabreiko, *Geometrical Methods of Nonlinear Analysis*, Springer-Verlag, Berlin/Tokyo, 1984.
- [32] R.S. Laugesen and M.C. Pugh, *Energy levels of steady states for thin-film-type equations*, J. Differ. Equat., **182** (2002), 377–415.
- [33] J.-L. Lions, *Quelques méthodes de résolution des problèmes aux limites non linéaires*, Dunod, Gauthier-Villars, Paris, 1969.
- [34] E. Mitidieri and S.I. Pohozaev, *Apriori Estimates and Blow-up of Solutions to Nonlinear Partial Differential Equations and Inequalities*, Proc. Steklov Inst. Math., Vol. **234**, Intern. Acad. Publ. Comp. Nauka/Interperiodica, Moscow, 2001.
- [35] C.V. Pao, *Nonlinear Parabolic and Elliptic Equations*, Plenum Press, New York, 1992.
- [36] L.A. Peletier and W.C. Troy, *Spatial Patterns. Higher Order Models in Physics and Mechanics*, Birkhäuser, Boston/Berlin, 2001.
- [37] L. Perko, *Differential Equations and Dynamical Systems*, Springer-Verlag, New York, 1991.

- [38] S.I. Pohozaev, *On an approach to nonlinear equations*, Soviet Math. Dokl., **20** (1979), 912–916.
- [39] S.I. Pohozaev, *The fibering method in nonlinear variational problems*, Pitman Research Notes in Math., Vol. **365**, Pitman, 1997, pp. 35–88.
- [40] P. Quittner and P. Souplet, *Superlinear Parabolic Problems and Their Equilibria*, Birkhäuser, 2007.
- [41] A.A. Samarskii, V.A. Galaktionov, S.P. Kurdyumov, and A.P. Mikhailov, *Blow-up in Quasilinear Parabolic Equations*, Walter de Gruyter & Co., Berlin, 1995.
- [42] A.E. Shishkov, *Dead cores and instantaneous compactification of the supports of energy solutions of quasilinear parabolic equations of arbitrary order*, Sbornik: Math., **190** (1999), 1843–1869.
- [43] D. Slepčev and M.C. Pugh, *Self-similar blow-up of unstable thin-film equations*, Indiana Univ. Math. J., **54** (2005), 1697–1738.
- [44] J.B. Van Den Berg and R.C. Vandervorst, *Stable patterns for fourth-order parabolic equations*, Duke Math. J., **115** (2002), 513–558.
- [45] M.A. Vainberg and V.A. Trenogin, *Theory of Branching of Solutions of Non-Linear Equations*, Noordhoff Int. Publ., Leiden, 1974.
- [46] T.P. Witelski, A.J. Bernoff, and A.L. Bertozzi, *Blow-up and dissipation in a critical-case unstable thin film equation*, Euro J. Appl. Math., **15** (2004), 223–256.
- [47] Ya.B. Zel'dovich, G.I. Barenblatt, V.B. Librovich, and G.M. Makhviladze, *The Mathematical Theory of Combustion and Explosions*, Consultants Bureau [Plenum], New York, 1985.

DEPARTMENT OF MATH. SCI., UNIVERSITY OF BATH, BATH, BA2 7AY, UK
E-mail address: `vag@maths.bath.ac.uk`